BNWL-1593
~~Special Distribution~~

Battelle
Pacific Northwest Laboratories
Richland, Washington 99352

AEC Research and Development Report

THE MTR-PHOENIX FUEL EXPERIMENT: CRITICAL TEST AND BURNUP RESULTS

J.W. Kutcher and E.C. Davis

June 1971

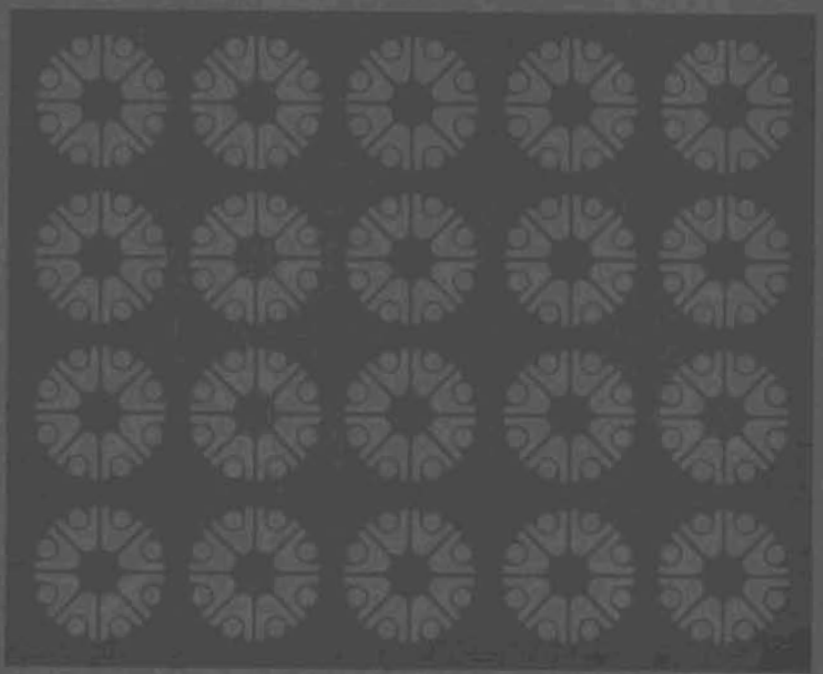

BNWL-1593

PACIFIC NORTHWEST LABORATORY
operated by
BATTELLE
for the
U.S. ATOMIC ENERGY COMMISSION
Under Contract AT(45-1)-1830

BNWL-1593

[redacted]

THE MTR-PHOENIX FUEL EXPERIMENT: CRITICAL TEST AND BURNUP RESULTS

By

J. W. Kutcher
E. C. Davis

June 1971

BATTELLE
PACIFIC NORTHWEST LABORATORIES
RICHLAND, WASHINGTON 99352

ABSTRACT

The MTR-Phoenix Fuel Experiment was a burnup experiment in the Materials Testing Reactor (MTR) with a plutonium-aluminum alloy fueled core, following a comprehensive set of critical experiments. This experiment utilized Phoenix fuel, a mixture of plutonium isotopes with a relatively high content of ^{240}Pu.

The work described in this report includes the loading of the MTR to critical with the Phoenix fuel core; the zero power measurements of shim rod and regulating rod worths, power distributions throughout the core, kinetic parameters, and reactivity worths of loss of coolant and loss of fuel plates; and the variation of some of the above parameters as the burnup of the core proceeded. The burnup history of the MTR-Phoenix core is also presented. The results are compared, where possible, with results obtained in the PRCF-Phoenix experiment and with calculations.

TABLE OF CONTENTS

LIST OF FIGURES

LIST OF FIGURES (CONTD) PAGE NO.

LIST OF FIGURES (CONTD) PAGE NO.

LIST OF TABLES

I. INTRODUCTION

The Phoenix Fuel Program at Pacific Northwest Laboratories (PNL) has as its primary objective the exploration and evaluation of the longer lifetime potential inherent in the use of the isotope ^{240}Pu as a burnable poison in nuclear reactor cores. The unusual property of ^{240}Pu as a burnable poison is that it converts to the fissile isotope ^{241}Pu upon absorbing a neutron. This is known as the Phoenix effect. Unlike ^{238}U, which is not produced during irradiation, ^{240}Pu is formed directly by non-fissioning neutron capture by the fissile isotope ^{239}Pu. The potential is therefore present for a reactor core design exhibiting a long endurance with relatively small reactivity change over the lifetime of the core.

Early survey work[1] singled out a small, high power density, water moderated core as the most likely vehicle for the Phoenix effect. Since the ultimate demonstration of the Phoenix effect would require a full scale core depletion experiment, and since the desired high power density, low core volume criteria were most nearly satisfied by the Materials Testing Reactor (MTR) type core, a burnup experiment was designed for the MTR itself.

A series of experiments was undertaken at PNL to provide support for the eventual burnup experiment in the MTR and to obtain more general integral information for pure plutonium systems. This campaign was conducted in four stages with decreasing generality as the MTR experiment became more firmly established:

1) Measurements of the infinite multiplication factor, k_∞, of arrays of borated polyethylene and Al-Pu alloy discs in the Physical Constants Testing Reactor (PCTR).[2]

2) Critical approach experiments with small cylindrical arrays of cans containing polyethylene and Al-Pu fuel discs in the Critical Approach Facility (CAF).[3]

3) Critical experiments in a mockup assembly designed to resemble the MTR reflector and projected Phoenix core in the Plutonium Recycle Critical Facility (PRCF).[4]

4) Startup critical experiments in the MTR with the Phoenix core prior to beginning the burnup experiment.

The data from each of these experiments have been analyzed[5] in turn - each step leading to further refinements in the analytical methods. These methods were used to perform a priori calculations for the MTR experiment, as reported in Reference 5.

The work described in this report includes the loading of the MTR to critical with the Phoenix fuel core; the zero power measurements of control system worths, power distributions throughout the core, kinetic parameters of the core, and loss of coolant - loss of fuel plates reactivity worths; and the variation of some of the above parameters as the burnup of the core proceeded. The results are compared, where possible, with results obtained in the PRCF-Phoenix experiment, and with calculations.

II. GENERAL DESCRIPTION OF MTR-PHOENIX FUEL CORE

The MTR[6,7] was a heterogeneous reactor, light water cooled and moderated, which used beryllium and graphite as a reflector. The fuel assemblies were plate type and were fabricated from aluminum. The core measured approximately 9 inches north to south by 28 inches east to west

by 24 inches high. Surrounding the core was a beryllium reflector which was 39 3/8 inches high and extended out to a diameter of 54 inches. Beyond this was a graphite reflector zone, which measured 12 feet north to south by about 15 feet east to west by 9 feet 4 inches high. The bottom of the graphite was located 4 feet below the core horizontal centerline.

The Phoenix core consisted of 19 fuel elements and 8 fuel-follower shim-safety rods located in the central 3 rows of the 5 x 9 lattice in the MTR, as shown in Figure 1. This represented a shift in position from the standard MTR uranium core, also shown in Figure 1.

The Phoenix fuel element, illustrated in Figure 2, was similar in design to the standard MTR fuel element in that all external dimensions were the same for both. The Phoenix element consisted of sixteen 0.080-inch thick, equally spaced plates curved to the MTR configuration. Each plate contained a 0.040-inch thick alloy core composed of 21 wt% plutonium and 79 wt% aluminum. Cladding was 6061 aluminum 0.020 inches thick.

Five of the elements were modified to contain flux monitors inserted down the inside corner beside the side plate and between the second and third fuel plates from the concave side and extending the full length of the plates. These flux monitors, illustrated in Figure 3, were Phoenix fuel wires, co-extruded with 1100 series aluminum clad, with end pieces welded on. The fuel content of each monitor was nominally 0.4 grams, and had the same isotopic composition as the fuel plates. The two adjacent fuel plates in the flux monitor assembly had narrower fuel cores than the standard plates, as shown in Figure 3.

The isotopic composition of the Phoenix fuel at the start of irradiation is listed in Table I.

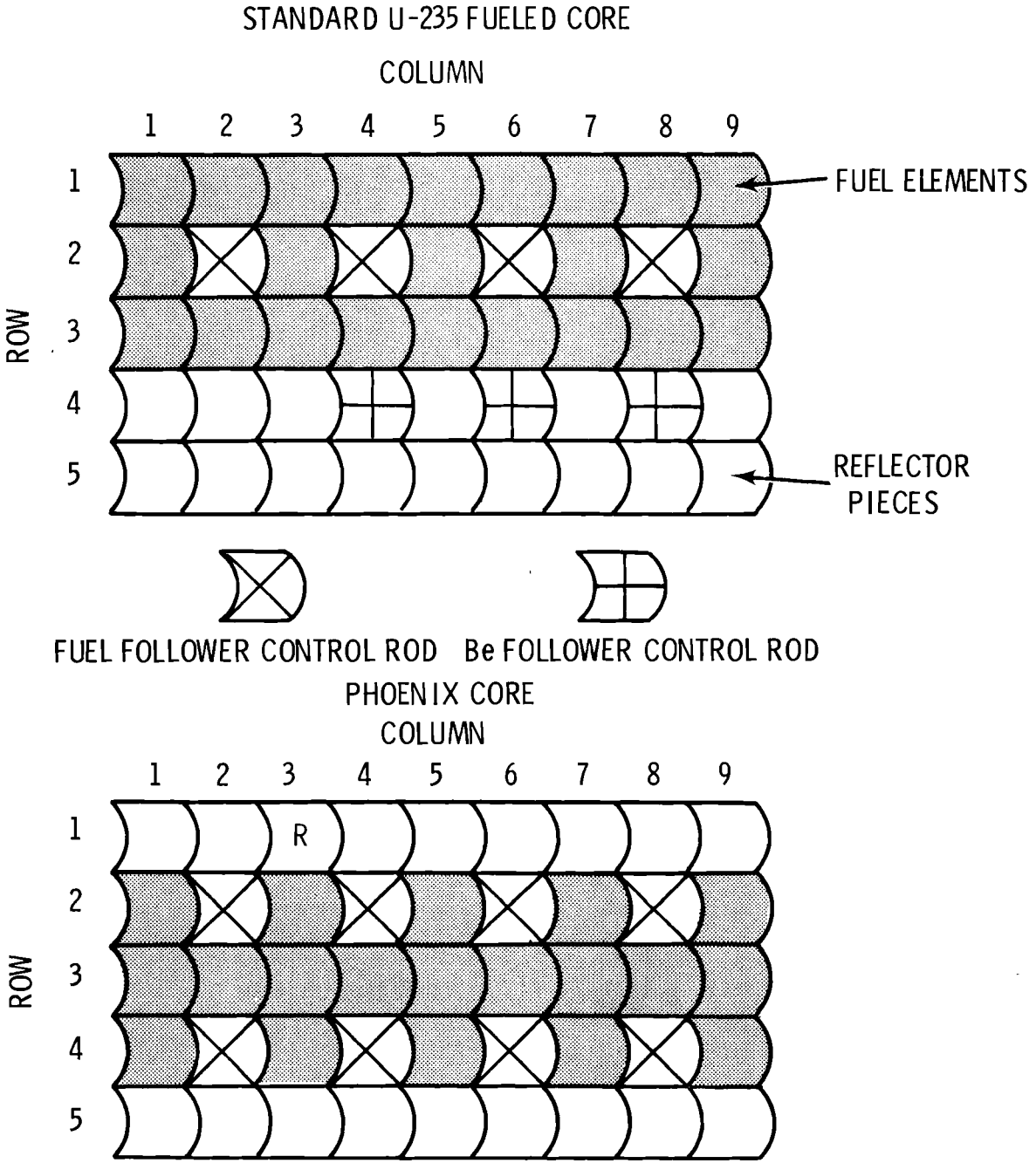

FIGURE 1. MTR Lattice Loadings for Standard and Phoenix Cores

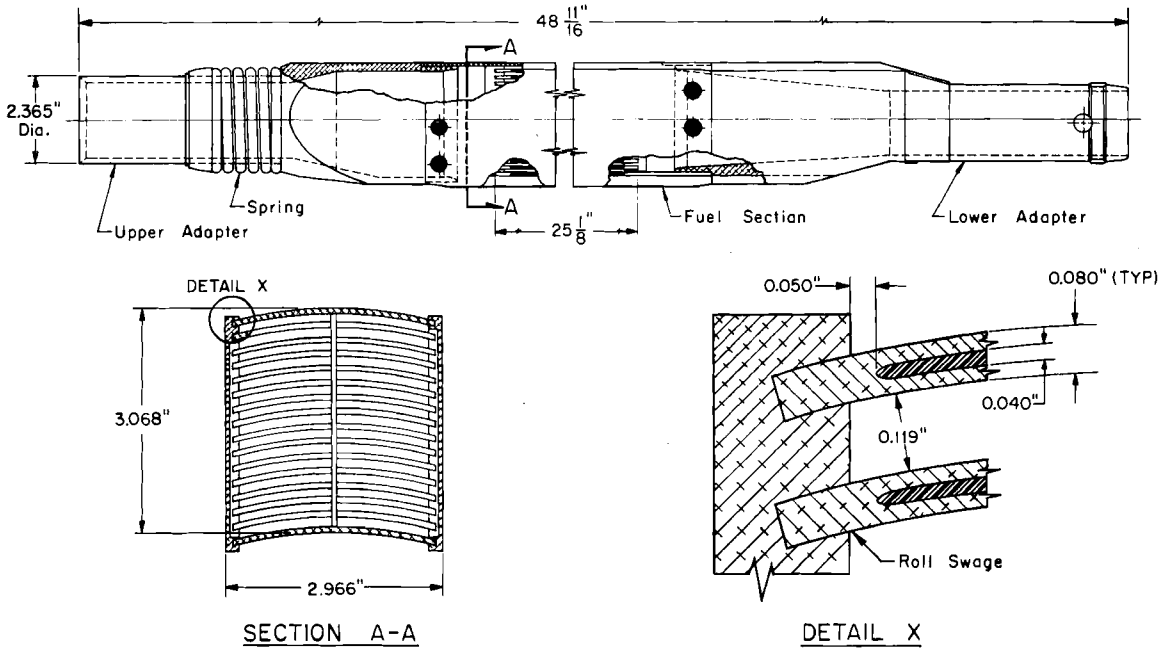

PHOENIX MTR FUEL ASSEMBLY

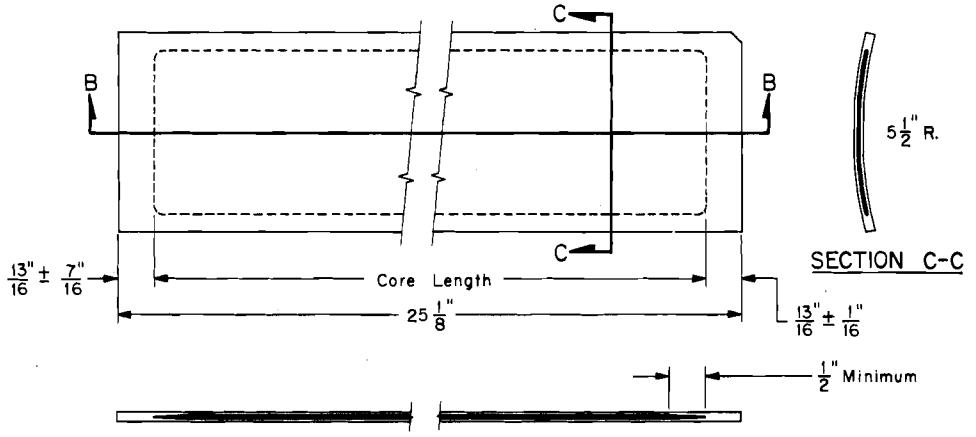

PHOENIX FUEL PLATE

FIGURE 2. MTR-Phoenix Fuel Element and Plate

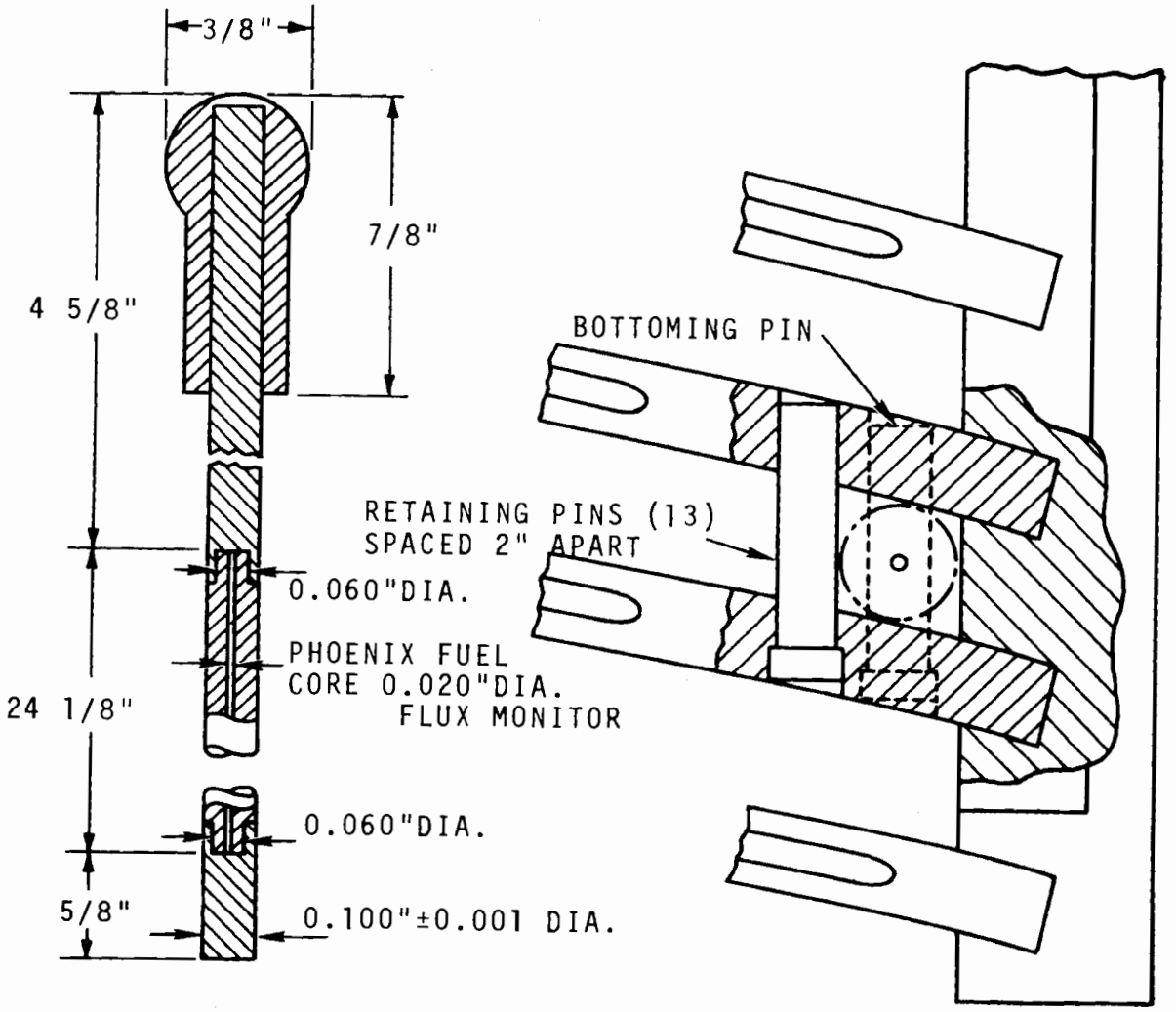

FIGURE 3. MTR-Phoenix Fuel Element with Flux Monitoring Position and Flux Monitor

TABLE I

PLUTONIUM ISOTOPIC CONCENTRATIONS IN PHOENIX FUEL

	Atom wt%.
^{238}Pu	0.539 ± 0.007
^{239}Pu	66.516 ± 0.055
^{240}Pu	23.201 ± 0.052
^{241}Pu	6.488 ± 0.034
^{242}Pu	3.257 ± 0.032

The cores of the standard fuel plates contained 24.4 ± 1.2 grams of plutonium while those for the narrow core plates contained 21.0 ± 1.1 grams of plutonium. The finished Phoenix fuel element contained 390 ± 5 grams of plutonium and the flux monitor element contained 384 ± 5 grams of plutonium.

The Phoenix shim safety (control) rods were physically similar to the standard MTR shim control rods with the major exception of thicker fuel plates in the fuel section. An assembly drawing is shown in Figure 4. Except for the fuel section, all remaining components (armature assembly, upper and lower aluminum sections, cadmium insert section, shock section, and associated hardware) were standard MTR components.

The fuel section of the Phoenix shim safety rod consisted of thirteen 0.080-inch thick plates of standard MTR configuration spaced with 0.110-inch water channels. The fuel plates utilized the same 0.040-inch thick alloy core composed of 21 wt% plutonium and 79 wt% aluminum as those in the regular fuel elements. The initial plutonium isotopic concentrations were those listed in Table I. The plutonium loading was 22.9 ± 1.1 grams per plate, or 298 ± 4 grams for the fuel section of one shim safety rod.

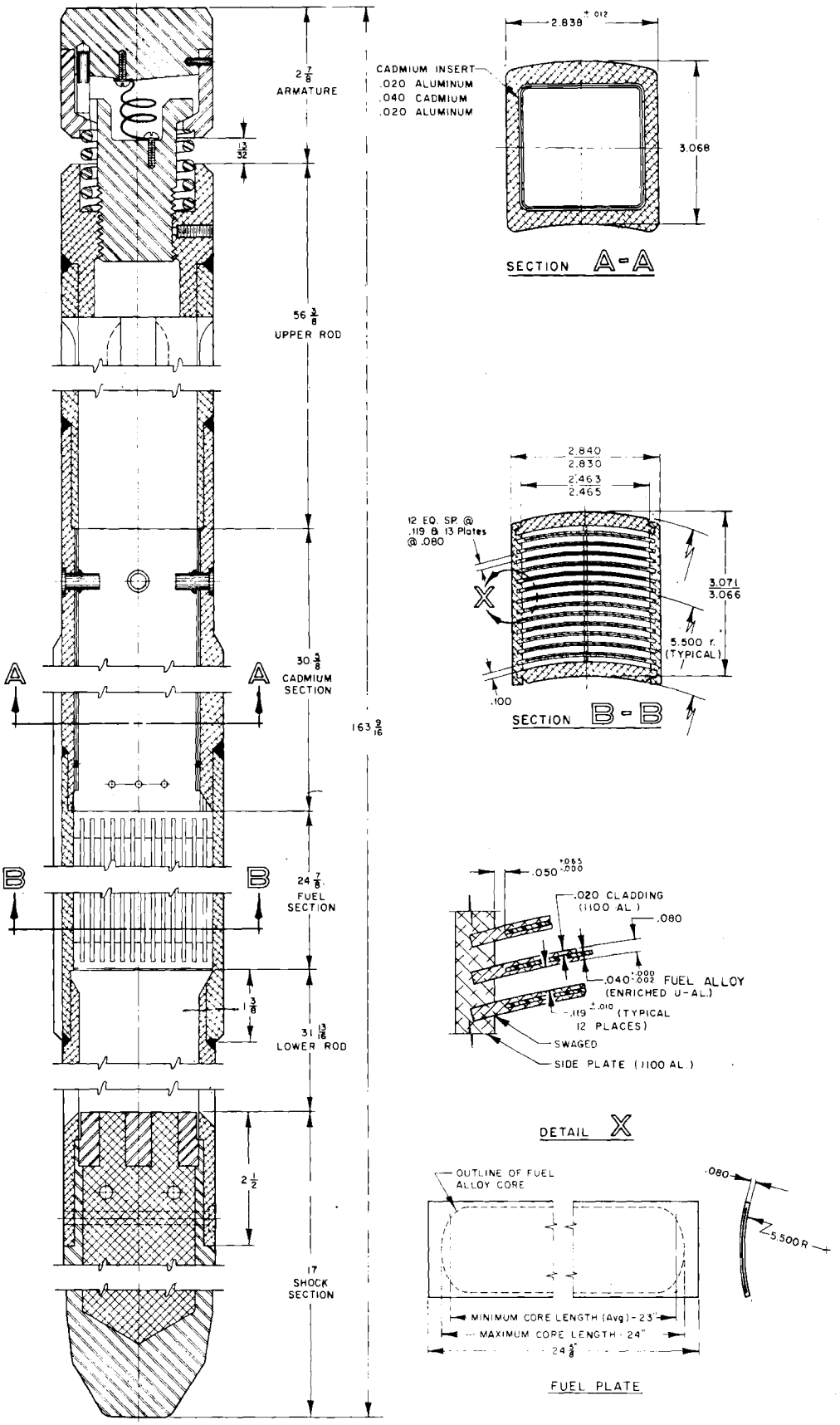

FIGURE 4. MTR-Phoenix Shim-Safety Rod

III. INITIAL STARTUP AND ZERO POWER EXPERIMENTS

A. Fuel Loadings

The first step of the Phoenix experiment in the MTR was the loading of sufficient fuel elements to form a critical array with all the shim-safety rods nearly withdrawn. All non-fueled positions in the 5 x 9 array contained beryllium reflector pieces. Initially four shim-safety rods with Be followers were positioned in lattice positions L-22, L-42, L-28, and L-48*. An antimony gamma source (providing neutrons from the Be) was installed in position L-32 for the approach-to-critical measurements.

The loading sequence of the Phoenix fuel is summarized in Table II. The loading was conducted in such a manner as to maintain a nearly complete Be reflector about the loaded fuel. In the first of these steps shim-safety rods with attached Phoenix fuel followers were installed in positions L-24, L-44, L-26, and L-46. Thereafter, all steps of both the approach-to-critical experiment and the post-critical loading consisted of fuel element insertions and the removal and reshuffling of Be lattice pieces.

For each configuration, count rate data were obtained at four rod bank heights: 0, 12, 21, and 30 inches of withdrawal (30 inches is the fully withdrawn position). These data were used to construct plots of reciprocal multiplication (1/M) as a function of total fuel content. The plot obtained with the rods 30 inches withdrawn was used to predict the initial critical loading. It was also compared with plots for each of the other bank heights to verify that the shim safety rod system had adequate shutdown capability.

*Lattice positions are indicated in Figure 1.

TABLE II

FUEL LOADING SCHEDULE FOR MTR-PHOENIX CORE

Fuel Loading Step	LB Piece Discharged From	L Piece Moved From	L Piece Moved To	Element or Shim Insertion Designation	Element or Shim Insertion Lattice Position	Incremental Pu Addition (g)	Total Pu Content of Core (g)
1	----	----	----	Shim NP-5	L-24	298.0	
	----	----	----	Shim NP-3	L-26	297.8	
	----	----	----	Shim NP-2	L-44	298.0	
	----	----	----	Shim NP-6	L-46	298.1	1191.9
2	----	----	----	Ele. MP-22	L-35	393.3	1585.2
3	L-38	L-25	L-38	Ele. MP-6	L-25	392.3	
	L-57	L-45	L-57	Ele. MP-3	L-45	389.7	2367.2
4	L-58	L-34	L-58	Ele. MP-4	L-34	394.4	2761.6
5	L-18	L-36	L-18	Ele. MP-2	L-36	393.2	3154.8
6	L-12	L-37	L-12	Ele. MP-1	L-37	389.2	3544.0
*7	L-32	L-33	L-32	Ele. MP-12F	L-33	386.6	3930.6
8	L-31	L-23	L-31	Ele. MP-11F	L-23	380.3	
	L-49	L-47	L-49	Ele. MP-9	L-47	392.4	4703.3
*9	L-52	L-43	L-52	Ele. MP-7	L 43	394.6	
	L-39	L-27	L-39	Ele. MP-8	L-27	393.8	5491.7
*10	L-21	L-32	L-21	Ele. MP-10F	L-32	384.5	
	L-29	L-38	L-29	Ele. MP-14F	L-38	384.0	6260.2
*11	Discharge rods with Be followers from L-22, L-48, L-42, and L-28			Shim NP-7	L-22	297.8	
				Shim NP-1	L-48	297.0	
				Shim NP-8	L-42	298.0	
				Shim NP-4	L-28	298.0	7451.0
*12	L-11	L-31	L-11	Ele. MP-19	L-31	387.2	
	L-19	L-39	L-19	Ele. MP-13F	L-39	383.3	8221.5
*13	L-51	L-21	L-51	Ele. MP-23	L-21	393.6	
	L-59	L-49	L-59	Ele. MP-18	L-49	396.3	
	----	L-29	Discharge	Ele. MP-16	L-29	393.3	
	L-41	----	----	Ele. MP-17	L-41	392.7	9797.4

*Critical configurations listed in Table III.

Criticality was achieved with a core loading of seven stationary fuel elements, four fuel-follower shim-safety rods, and four beryllium-follower shim-safety rods as shown in Figure 5. The critical rod bank height for this configuration was 28.853 inches. From rod calibration data (see following section) it was determined that k = 1.002 for all eight shim-safety rods full out. This compares with a calculated value of k = 1.016 as reported in reference 5.

Post-critical fuel loadings were also made according to the schedule in Table II. Following each fuel loading step, the reactor was made critical, the banked rod positions recorded, and the adequacy of the shut-down margin verified. These additional configurations are shown in Figure 5. The banked rod position and the inferred rods-out reactivity for each step are listed in Table III.

TABLE III

CRITICAL CONFIGURATIONS FOR MTR-PHOENIX CORE

Fuel Loading Step*	No. of Stationary Fuel Elements	No. of Fuel-Follower Shims	No. of Beryllium-Follower Shims	Critical Rod Bank Height	Inferred Rods Out k_{eff}	Calculated[5] Rods Out k_{eff}
7	7	4	4	28.853	1.002	1.016
9	11	4	4	21.40	1.057	1.070
10	13	4	4	20.30	1.071	1.085
11	13	8	-	19.00	1.089	1.086
12	15	8	-	18.75	1.093	1.096
13	19	8	-	18.03	1.104	1.113

*Refer to Table II

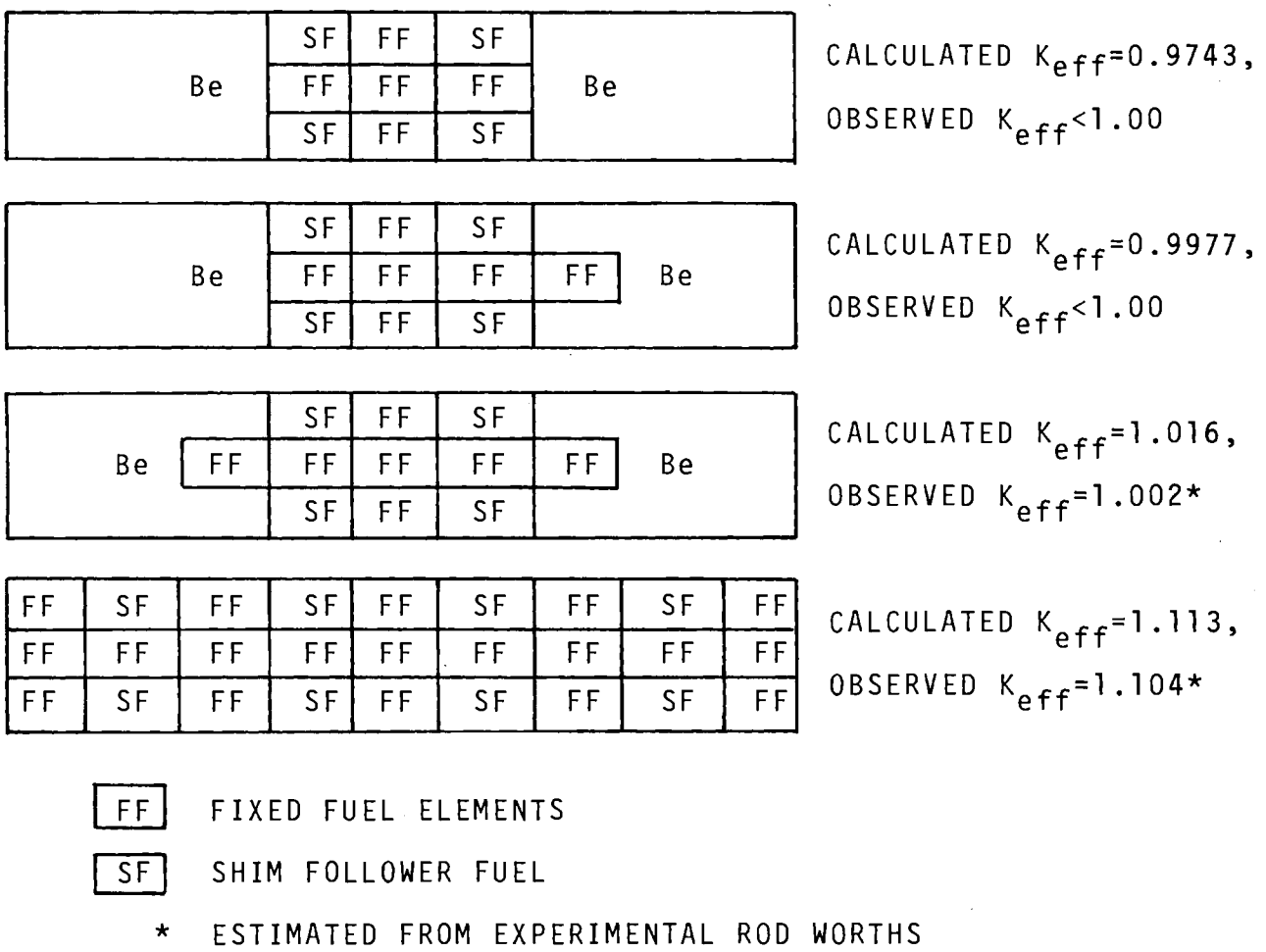

FIGURE 5. MTR-Phoenix Critical Loading Sequence

B. Rod Calibrations

Reactivity calibrations were performed on all eight fuel-follower shim-safety rods in the MTR-Phoenix core. One exterior rod (L-48) and one interior rod (L-46) were calibrated over their full 30-inch travel. The relative worths of the remaining six rods were determined by measuring the reactivity worth of 1 to 2 inches of withdrawal for each rod.

The technique used for these calibrations employed the movement of the rod in calibration, the measurement of the associated stable reactor period, and the interpretation of that period in terms of reactivity using the inhour equation. All rod calibrations were performed one rod at a time, inserting all remaining shim-safety rods as a bank (± 1.5 in. of their mean position) to re-establish criticality. The mean position of these banked shim-safety rods was not permitted to be less than 12.5 inches.

The shim-rod differential worths, measured at a height of 18 inches, are listed in Table IV.

TABLE IV

INITIAL SHIM ROD DIFFERENTIAL WORTHS

Shim Rod	Worth (¢/in.)*
L-22	61.8 ± 1.4
L-42	61.6 ± 1.4
L-24	91.0 ± 2.0
L-44	91.4 ± 2.0
L-26	92.2 ± 2.0
L-46	90.6 ± 2.0
L-28	45.7 ± 1.0
L-48	58.6 ± 1.3

*All reactivity worths measured at a height of 18 inches.

The total integrated worth for the interior rod L-46 was determined to be \$16.5, or 44.6 milli-k. The integrated worth for the exterior rod L-48 was \$9.5, or 25.7 milli-k. The total worth of the entire 8-rod bank was inferred to be \$101, or 274 milli-k. The integrated worth of the 8-rod bank appears in Figure 6.

The phenomenon of reactivity worth reversal which was observed in the PRCF-Phoenix Experiment[4] was also noted in the MTR. This phenomenon is believed to result from moving the lower end of the fuel follower out of the region of high thermal neutron flux just below the core, while the upper part of the fuel follower is being moved into the region at the top of the core where the flux is severely depressed by the banked shims. The integrated worth of L-46 reached \$17.4 (47.0 mk) before the reversal lowered it to \$16.5, while L-48 reached a peak integrated worth of \$9.95 (26.9 mk).

The regulating rod for the MTR-Phoenix core was located in the reflector in lattice position L-13 (see Figure 1). This rod is designed to be moved by a servo system to provide automatic control of the reactor power. The reactivity worth of the regulating rod was required to be small enough that rapid withdrawal of the rod could not cause a transient which would damage the core and large enough that the rod could control reactor power during routine operation. These requirements were met by setting an upper limit of \$1.20 and a lower limit of \$0.30 on the regulating rod worth.

The rod tested initially had 0.040-inch cadmium sheets arranged on a 1.195-inch diameter, covered by a stainless steel sleeve. The total

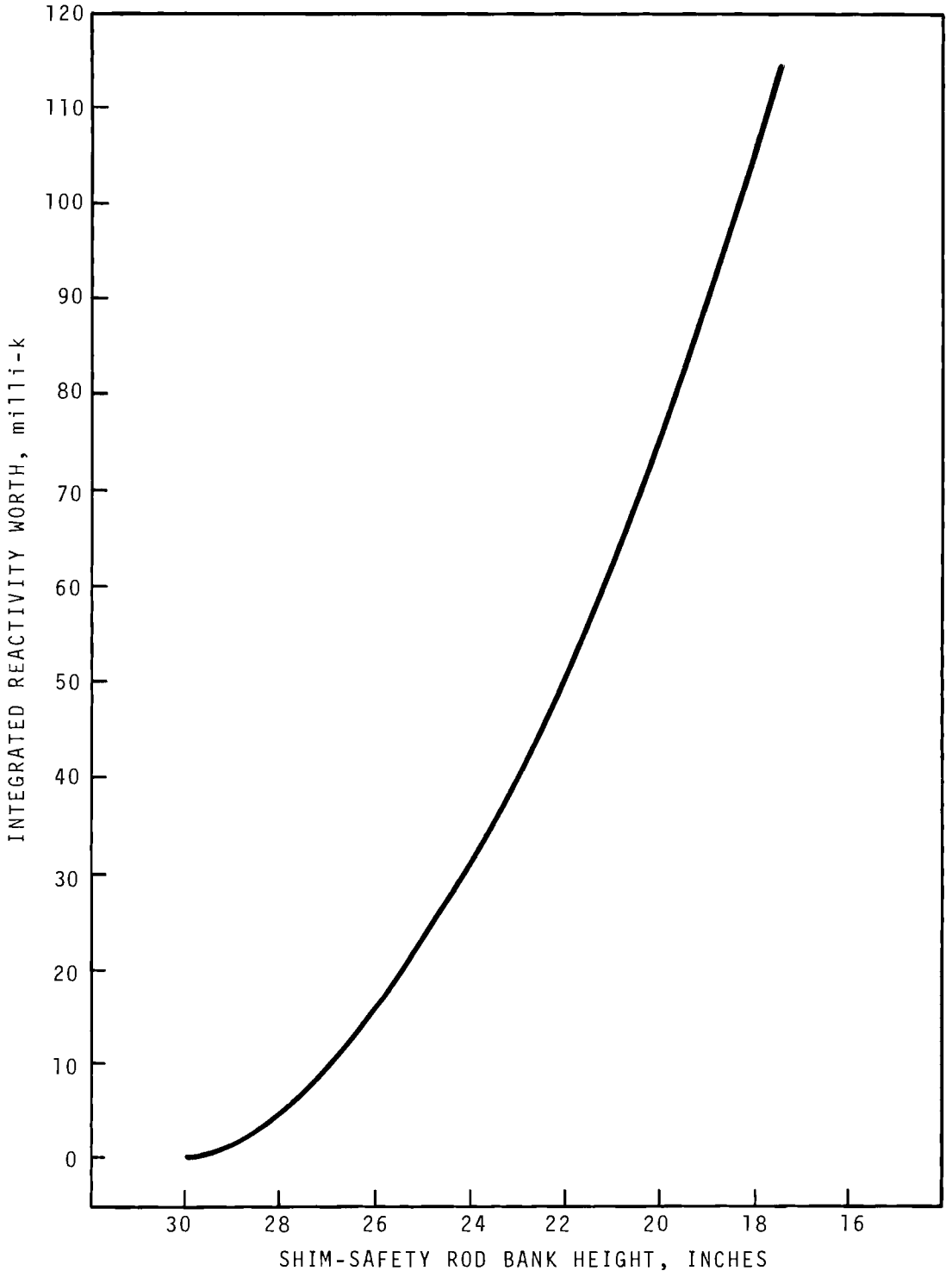

FIGURE 6. Reactivity Worth of Shim-Safety Rod Bank

worth of this rod was measured to be $1.65, which was excessive. A second rod was built with a 1.110-inch diameter and an aluminum sleeve. The total worth of this rod was $1.60. Finally, a rod was constructed with the cadmium sheets on a 0.50-inch diameter. The total worth of this rod was measured to be $1.02, so this rod was employed throughout the burnup of the MTR-Phoenix core.

C. Power Distribution Measurements

Power and fission-rate distribution data for the MTR-Phoenix core were obtained in a series of five irradiations (flux runs). These data were important in determining the maximum reactor power level as well as providing experimental data for comparison with calculations. The distributions were determined by gamma scanning ^{235}U pins, Pu wands, and removable fuel plates.

Two demountable MTR-Phoenix fuel elements were available for use in these low-power irradiations. Alternate fuel plates were removable from each of these elements. These plates were gamma scanned following irradiation to obtain individual fuel plate power distributions. The power generation in the element was then inferred by plotting these measured plate powers as a function of position in the element and assigning powers to the fixed plates by interpolation.

Relative powers from element to element were determined from the activity of ^{235}U wires which were taped to plastic wands located in water channel No. 8 of each element. At least four ^{235}U wires were used in each element. Data from the various irradiations were inter-normalized using the axial fission-rate distribution measured in L-34 with ^{235}U wires in each irradiation.

A comprehensive analysis of the results of all the fuel plate gamma scans and ^{235}U pin activity data was made to derive a detailed power map for the MTR-Phoenix core. This analysis required the correlation of the experimental data from throughout the core and the determination of the unique power shapes for each box for all core positions. The percent of core power for each fuel element is presented in Figure 7, along with the uncertainties on each value. The methods used for determining the box power for each fuel element, as listed in Figure 7, are summarized in Table V.

TABLE V

DETERMINATION OF FUEL ELEMENT POWERS

Fuel Element	Determined	Method
Fixed Elements:		
L-31, 35, 36, 37, 39, 45, 47, 49	Measured	Pu fuel plate gamma scanning
L-21, 23, 27, 29 34, 36, 41, 43 47, 49	Measured	^{235}U pin activity data
L-33	Estimated	Ratio of adjacent and symmetrical fixed elements
L-32, 38	Estimated	Interpolated from adjacent fixed elements
Shim-Follower Elements:		
L-46	Measured	Pu wand gamma scanning
L-22, 24, 26, 28 42, 44, 46, 48	Estimated	Average of adjacent fixed elements all ratioed to measured power in L-46

	1	2	3	4	5	6	7	8	9
2	2.90 ±0.07	3.22 ±0.16	4.04 ±0.13	4.43 ±0.20	5.18 ±0.15	4.43 ±0.20	4.06 ±0.16	3.12 ±0.16	2.69 ±0.10
3	2.66 ±0.04	3.22 ±0.24	3.38 ±0.14	4.79 ±0.15	4.87 ±0.13	4.76 ±0.11	3.34 ±0.05	3.11 ±0.19	2.50 ±0.04
4	2.86 ±0.07	3.17 ±0.16	3.95 ±0.13	4.34 ±0.19	5.00 ±0.08	4.32 ±0.15	3.91 ±0.07	3.07 ±0.14	2.70 ±0.04

FIGURE 7. Percent Power per Fuel Element in the MTR-Phoenix Core

The MTR-Phoenix core power map shown in Figure 7 was reduced to quarter-core symmetry to compare it with the power map from the PRCF-Phoenix core.[4] This comparison appears in Figure 8, where the values are given in percent power per element. One can see from the figure that the power distribution in the MTR is somewhat more peaked toward the center of the core than it was in the PRCF. The effect of the better side reflector in the MTR may also be seen. End leakage was higher in the MTR; side leakage was higher in the PRCF.

A large body of data was obtained from the gamma scanning of removable fuel plates. Shown in Figure 9 are the results of full-width axial scans of two plates from the element irradiated in position L-45. The outside plate (No. 16) is seen to have a more peaked power distribution (normalized to the core average power) than the inside plate (No. 8). The peak power on plate No. 16 is 2.64 times the core average.

The results of all the full-width axial plate scans performed in this experiment appear in an appendix to this report.

Figure 10 shows the plate-to-plate power distributions in all eight core positions for which gamma scanning was done. All data are presented as plate average power normalized to core average power.

Power distribution data were needed in the shim-safety rod in position L-46 to insure that burnout would not be inadvertently obtained in a fuel-follower section during full-power operation. A spare shim-safety rod was modified to allow positioning of ^{235}U wires in the water channels of the fuel-follower section. Those wires were inserted in plastic wands, as shown in Figure 11.

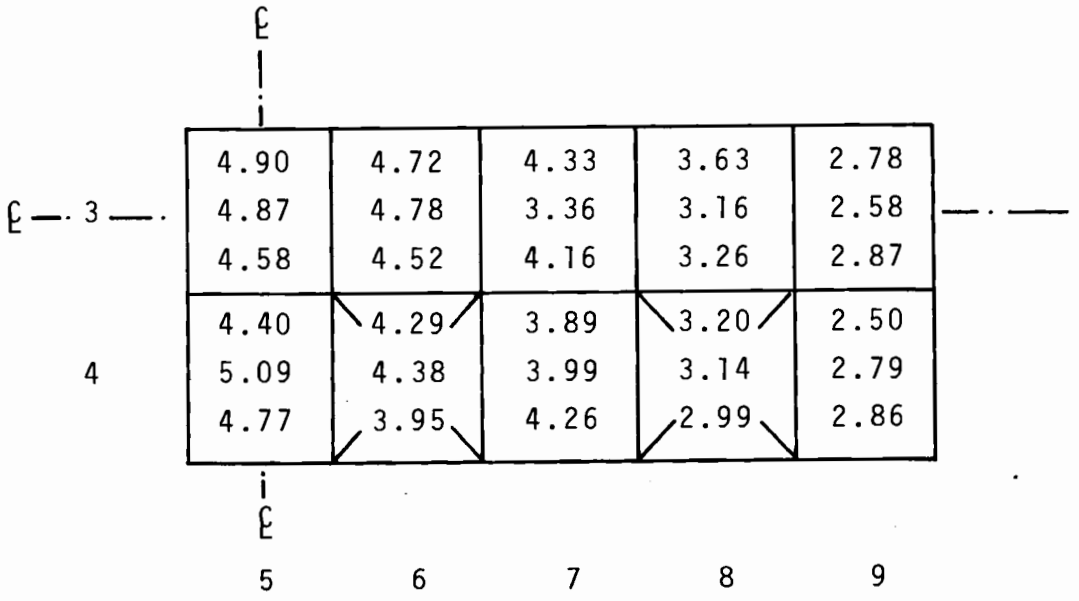

PERCENT POWERS:
1. CALCULATED FOR MTR-PHOENIX CORE
2. MEASURED IN MTR-PHOENIX CORE
3. MEASURED IN PRCF-PHOENIX CORE

FIGURE 8. Quarter Core Power Map Comparison: MTR-Phoenix Core and PRCF-Phoenix Core

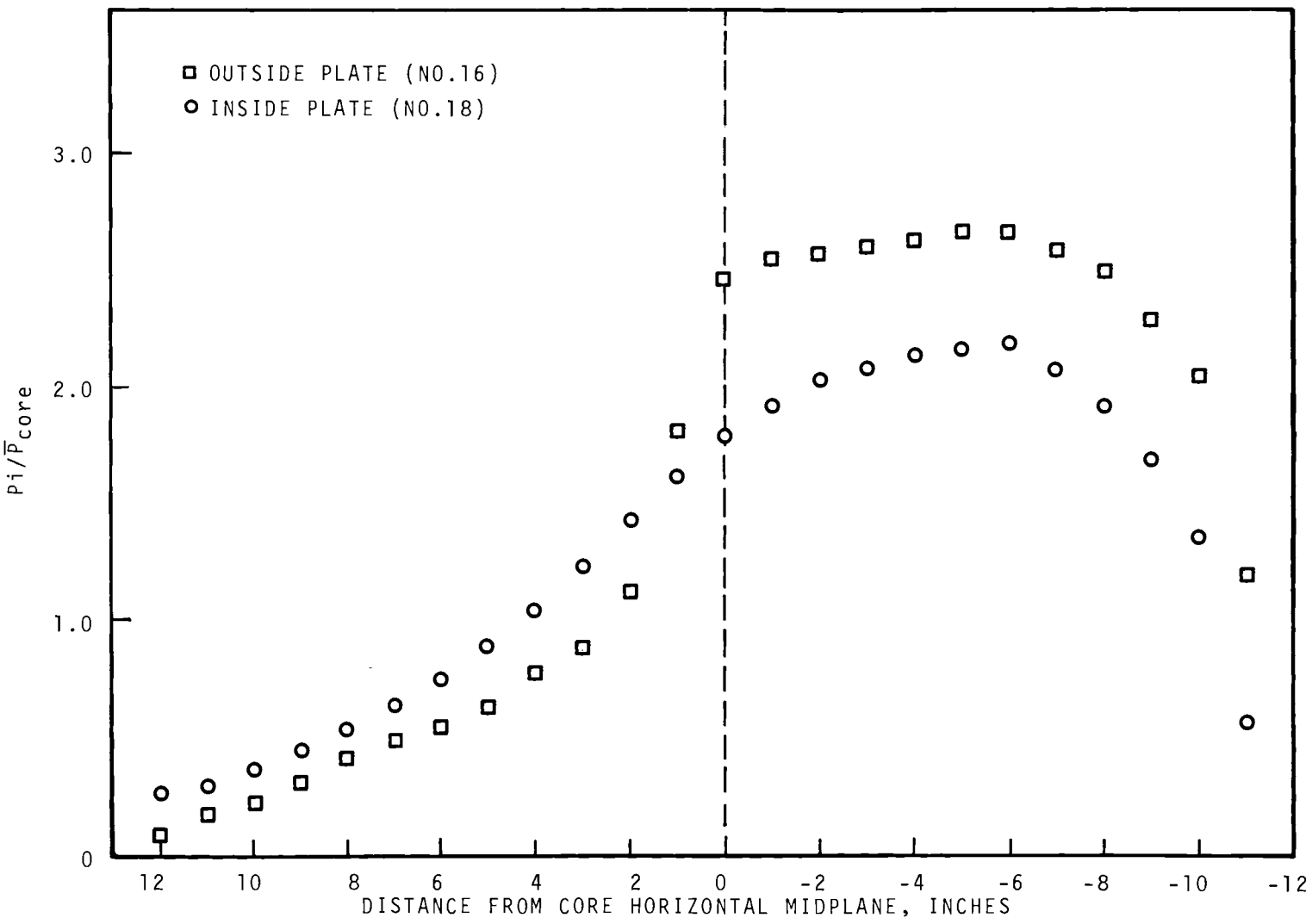

FIGURE 9. Full-Width Axial Gamma Scans of Two Plates from Fuel Element Position L-45

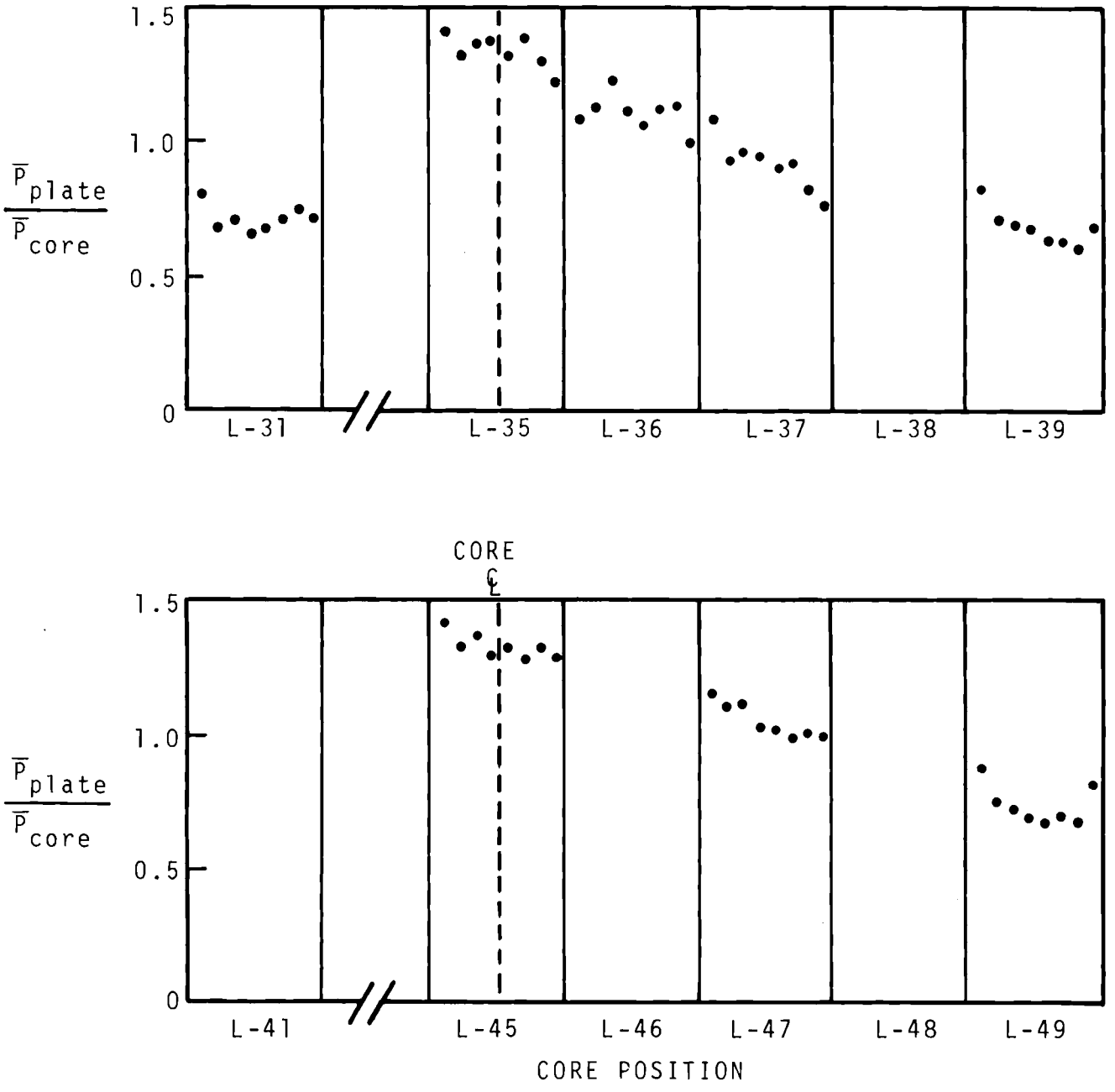

FIGURE 10. Fuel Plate Average Power Map of the MTR-Phoenix Core

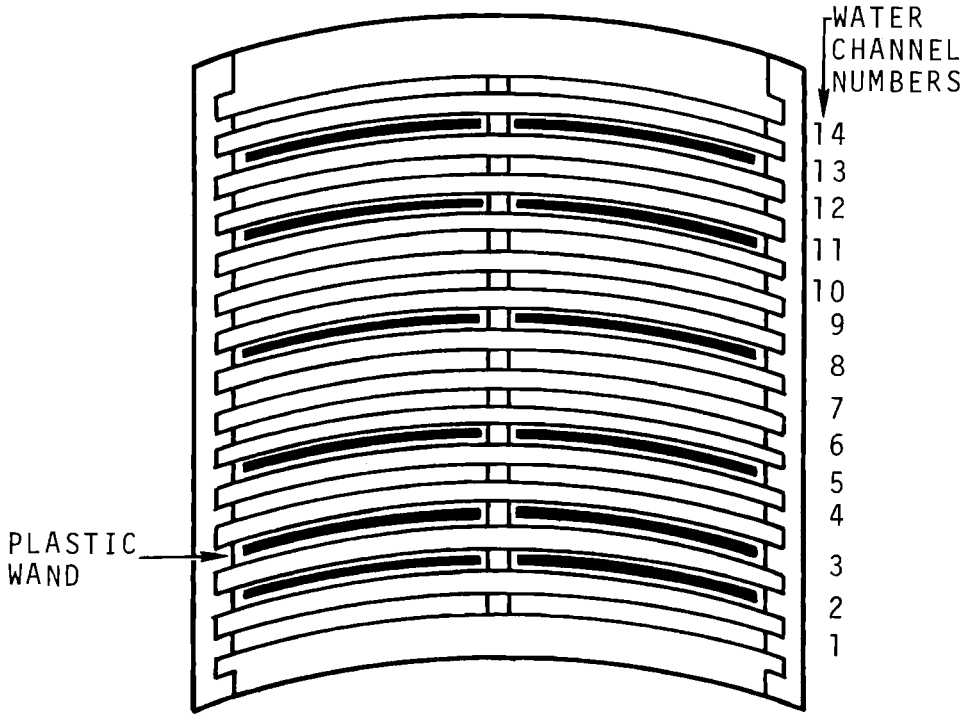

FIGURE 11. Cross-Sectional Diagram of MTR-Phoenix Fuel-Follower Section Showing Location of Plastic Wands for Positioning ^{235}U Wires

A problem arose in connection with the ^{235}U activation results and necessitated an additional irradiation. The axial scan of a ^{235}U pin irradiated in channel No. 8 of the fuel element in position L-45 yielded results different from those obtained from an axial scan of plate No. 8 in this element. These results are shown in Figure 12. Calculations failed to account for this discrepancy. Since power distribution measurements in the shim-follower had been made exclusively with ^{235}U wires, these results became suspect. Accordingly, an irradiation was performed with several plutonium flux wands inserted in the water channels of the fuel-follower section. The results of these measurements are shown in Figure 13.

At the same time a plutonium flux wand was irradiated in position L-45. The result of this measurement appears in Figure 12. It can be seen that the Pu wand data agree much more closely with the Pu plate data than with the ^{235}U pin data. Hence, the Pu wand data were used to determine power distributions in the shim fuel-follower.

The peak power in the MTR-Phoenix core was inferred from the data to occur on plate No. 1 of the shim fuel-follower in position L-46. The ratio of this peak power to the core average was 4.28 ± 0.52. This peak limited reactor power to 24 MW, based on heat removal considerations.

D. Void and Loss-of-Fuel Measurements

Measurements were made of the reactivity effects associated with void formation and loss of fuel plates in the highest worth element in the core. These experiments were designed to provide a correlation with the extensive studies of these void and fuel removal effects conducted

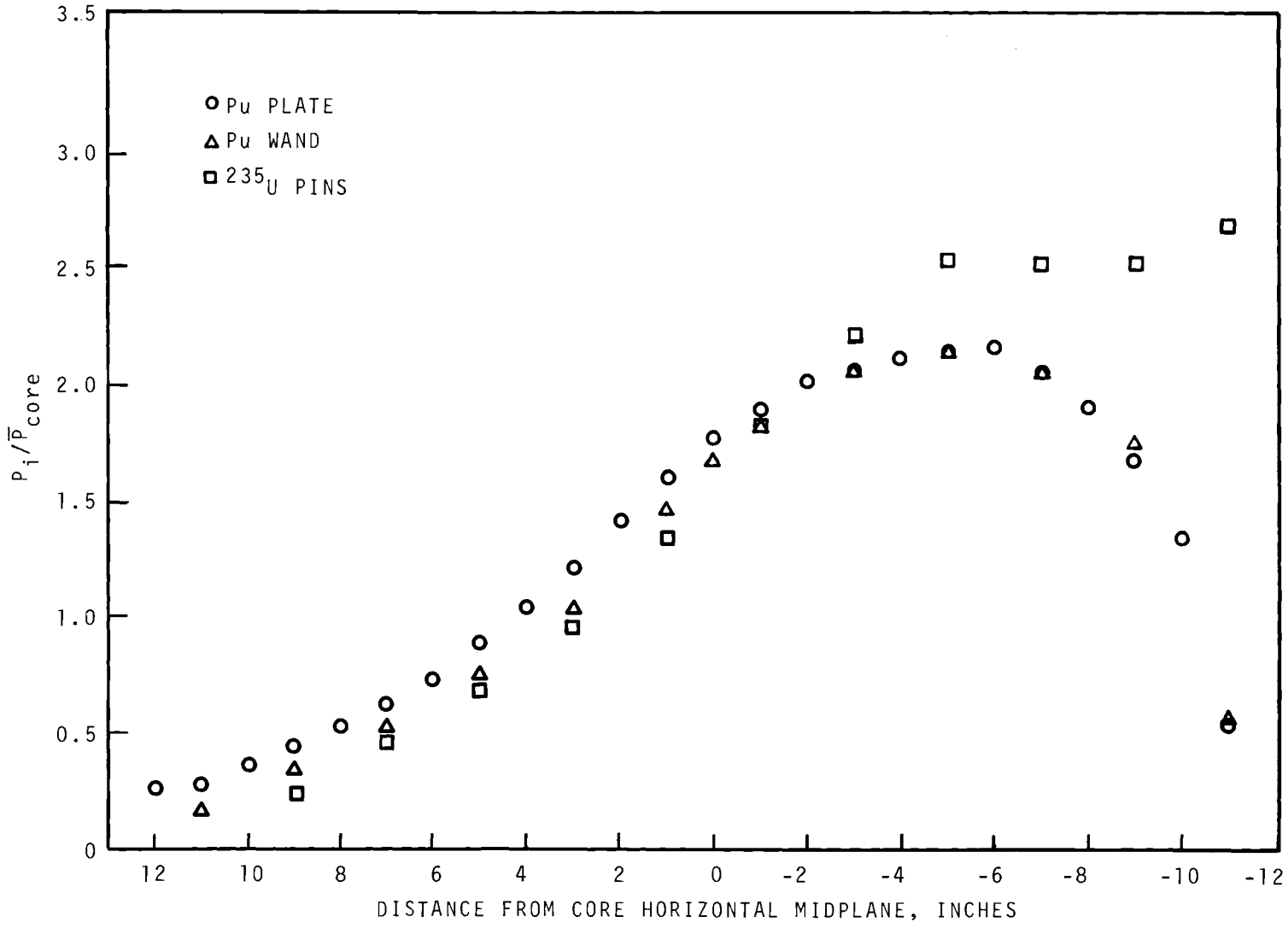

FIGURE 12. Axial Power Distribution in Fuel Element Position L-45: Pu Plate Vs. Pu Wand Vs. ^{235}U Pins

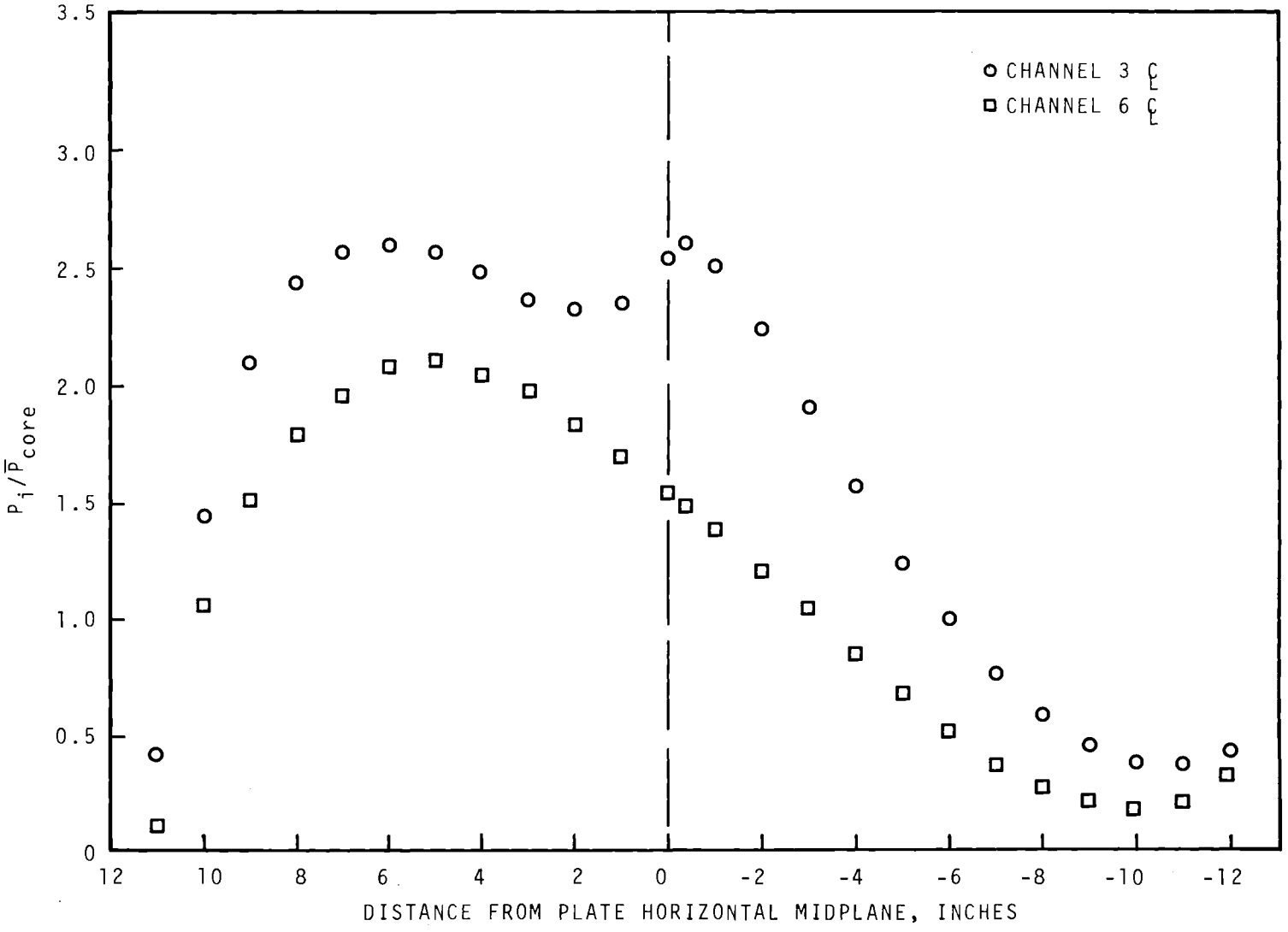

FIGURE 13. Axial Scans of Pu Wands Located in Water Channels of Shim Fuel-Follower in Position L-46

in the PRCF,[4] as well as to confirm the calculated effects reported in the safety analysis report.[7] For the MTR-Phoenix core, the reactivity effects were simulated in a demountable fuel element, and a critical run was made both with and without the simulated effect. The reactivity change due to the simulated effect was calculated from the change in critical position of a previously calibrated shim-safety rod.

In order to study void formulation, a full channel width teflon strip (full core length) was positioned in channel No. 8 of a demountable element, with the element inserted in position L-35. This was the channel in the very center of the Phoenix core, and was therefore expected to have the largest reactivity worth. The measured reactivity effect of this "void" was -18.7 ± 2¢. The measured effect in the same channel of the PRCF-Phoenix core was -23.6 ± 2¢, so the results are seen to be comparable.

Since the temperature effect on reactivity in the MTR-Phoenix core was due in large part to the reduction of coolant water density, it is possible to infer a temperature coefficient of reactivity from the measured effect of a coolant void. The inferred temperature coefficient of reactivity for this core was -1.3¢/°C, slightly smaller than the value of -1.85¢/°C predicted in the safety analysis report.

The reactivity effect of fuel plate removal also required the use of a demountable element. The effect studied was the loss of plate No. 8 from an element installed in position L-35. The reactivity change due to removing this plate was measured to be +33.4 ± 2¢. The comparable measurement in the PRCF yielded a reactivity change of +34.0 ± 2¢, so the two cases show remarkable agreement. The positive effect of replacing a

fuel plate with water is, of course, due to the fact that the Phoenix is very undermoderated. In the PRCF positive incremental worths were obtained up to and including three plates removed. Removal of a fourth plate had a slightly negative incremental worth.

A measurement was made of the effect of removing plate No. 16 in position L-45. This was a plate which calculations had indicated as a likely candidate for the core hot spot, so the effect of its removal was of some interest from the viewpoint of safety. The reactivity change due to removing this plate was measured to be -1.7 ± 2¢.

E. Kinetics Measurements

Reactor noise measurements were made with low-flow and zero-power reactor operating conditions to determine the value of the ratio β/ℓ - the effective delayed-neutron fraction divided by the prompt-neutron lifetime. Noise data were recorded using both ^{3}He and fission chambers. The signals from the chambers were recorded on magnetic tape during the measurement, and subsequently analyzed to determine power spectral density from which the ratio β/ℓ was obtained.

The best results were obtained from a sixty-minute recording of the ^{3}He neutron detectors. The cross power noise spectrum obtained is shown in Figure 14.[8] The cross spectral density function yielded a β/ℓ break frequency of 9.23 ± 0.11 Hz.

A twenty-five minute recording of fission chamber signals was also analyzed. This shorter record length cross spectrum yielded a best estimate of β/ℓ of 9.43 ± 0.30 Hz.

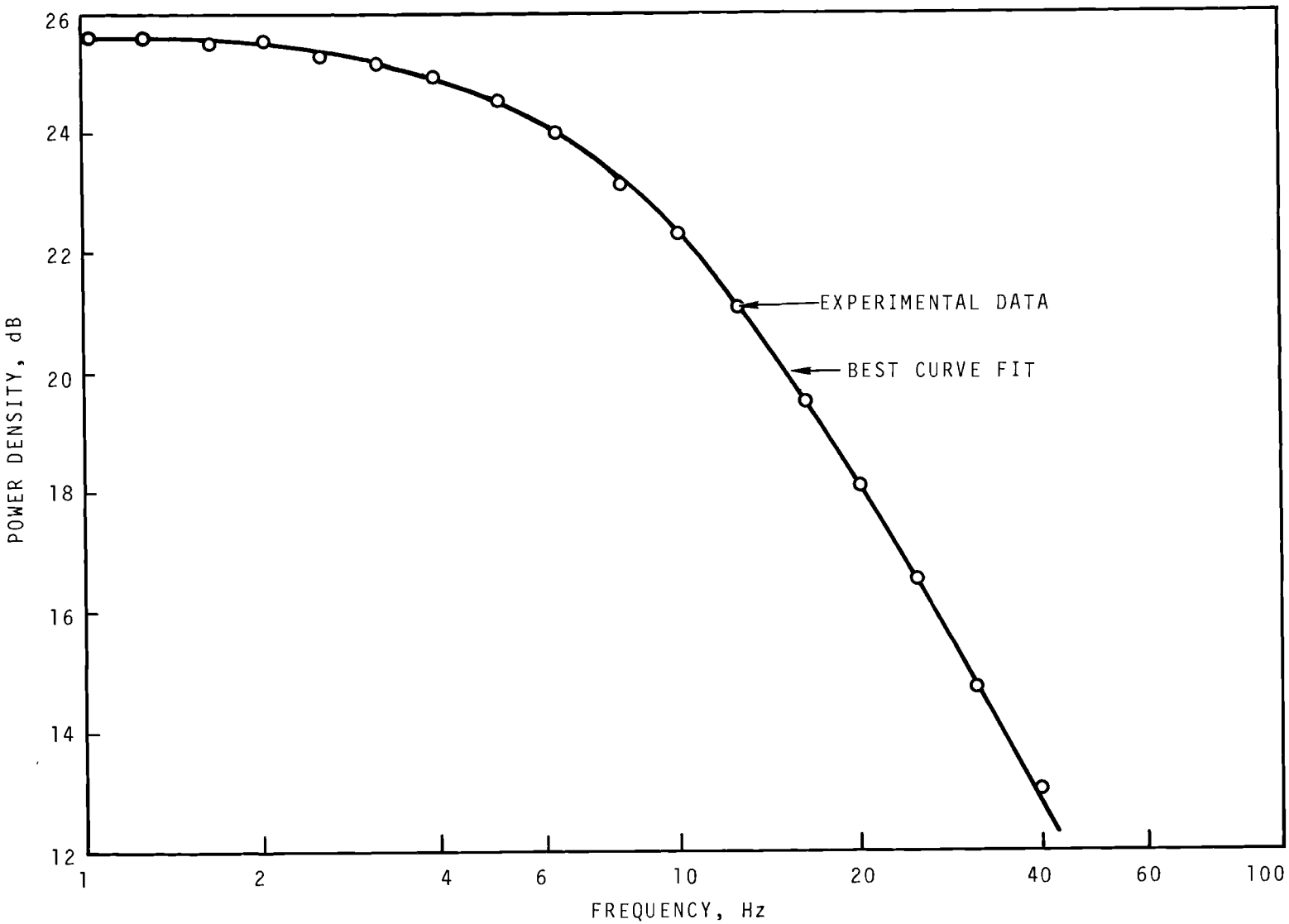

FIGURE 14. Cross Power Noise Spectrum: MTR-Phoenix Core with Zero Burnup

By comparison, data recorded from BF_3 chambers in the center of the PRCF-Phoenix core yielded a β/ℓ break frequency of 9.45 ± 0.11 Hz.[4]

IV. BURNUP HISTORY

Following the completion of the critical experiments described in the previous section, the burnup experiment began. Power operation began before final evaluation of the power distribution data so that initial operation was at lower powers than the 24 MW mentioned in the previous section. Eventually, reactor power did reach a maximum of 24 MW. After about 70% of the MTR-Phoenix core burnup had been obtained, operating power was reduced to 12 MW in order to prolong the calendar life of the MTR operation. The power history of the MTR-Phoenix core appears in Figure 15. The MTR was operated on a five-day week after March 1, 1970; this accounts for the frequency of startups and shutdowns.

The normal mode of equilibrium power operation was to compensate for the gradual loss of reactivity by moving the regulating rod from its least reactive position to its most reactive position. The regulating rod was then returned to its least reactive position in conjunction with a withdrawal of the banked shim-safety rods. During steady operation these rods were always operated as a bank. Rod bank height positions as a function of core burnup are shown in Figure 16 and listed in Table VI. All these positions were measured at equilibrium power and fission product posioning.

Using shim-rod calibration data, the rod bank height position was converted into the value of k_{eff} with all rods withdrawn. The rods-out k_{eff} as a function of core burnup is plotted in Figure 17. Again, all these values are at equilibrium power. The total burnup of the MTR-Phoenix core was 923 MWd.

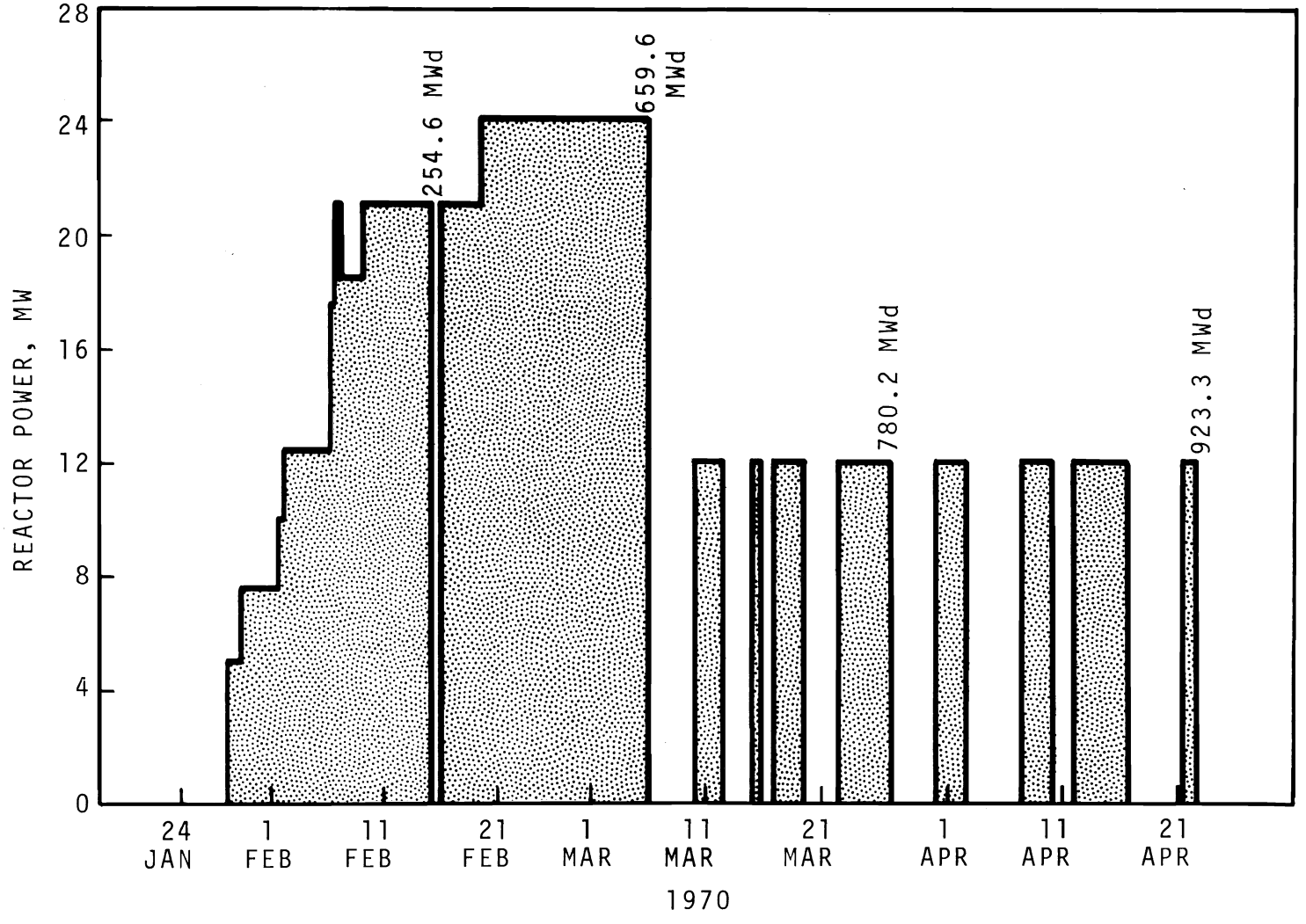

FIGURE 15. MTR-Phoenix Core Power History

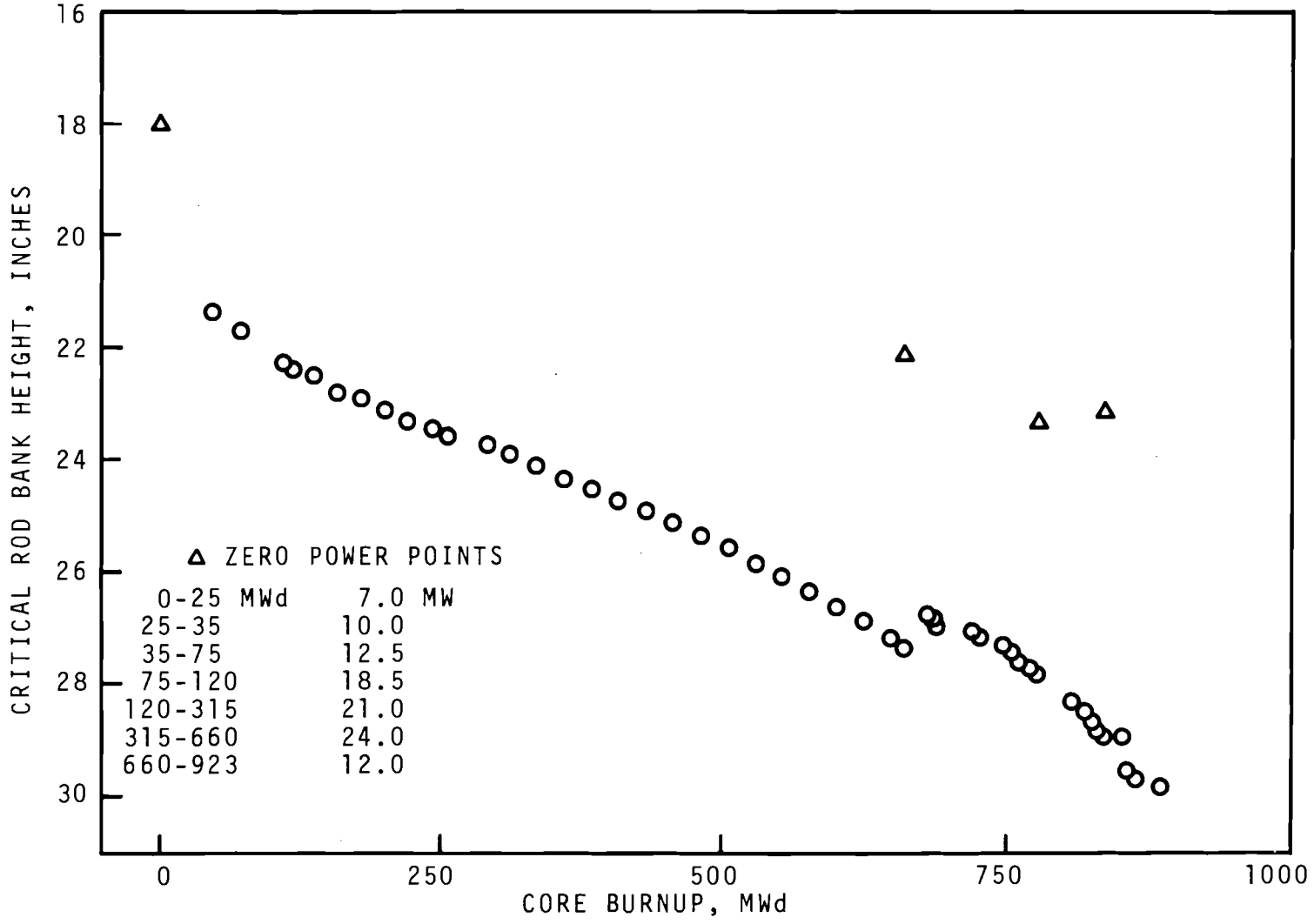

FIGURE 16. Critical Rod Bank Height at Equilibrium Power Vs. MTR-Phoenix Core Burnup

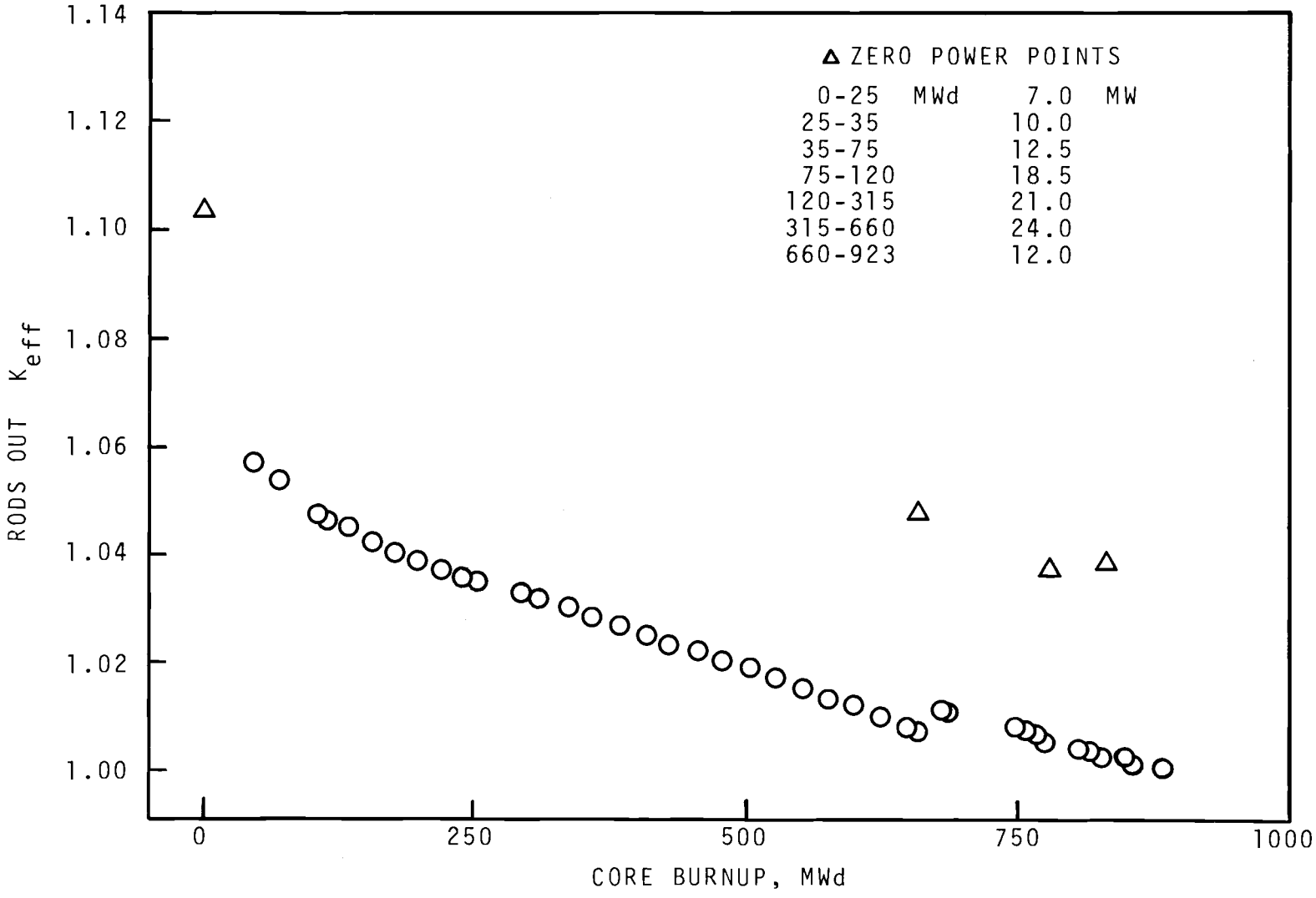

FIGURE 17. Rods-Out K_{eff} Vs. MTR-Phoenix Core Burnup

TABLE VI

MTR-PHOENIX BURNUP DATA

Core Burnup (MWd)	Equilibrium Power (MW)	Shim Rod Bank Height (in)	Rod-Out Reactivity k_{eff}
0	0	18.026	1.104
46.0	12.5	21.320	1.057
70.9	12.5	21.680	1.054
106.8	18.5	22.251	1.047
115.9	18.5	22.389	1.046
135.6	21.0	22.485	1.045
156.6	21.0	22.790	1.042
177.6	21.0	22.915	1.040
198.6	21.0	23.125	1.039
219.6	21.0	23.310	1.037
240.6	21.0	23.460	1.036
254.6	21.0	23.565	1.035
291.3	21.0	23.725	1.033
312.3	21.0	23.913	1.032
335.9	24.0	24.135	1.030
359.9	24.0	24.350	1.028
383.9	24.0	24.545	1.027
407.9	24.0	24.745	1.025
431.9	24.0	24.940	1.023
455.9	24.0	25.150	1.022
479.9	24.0	25.360	1.020
503.9	24.0	25.575	1.019
527.9	24.0	25.860	1.017
551.9	24.0	26.090	1.015
575.9	24.0	26.335	1.013
599.9	24.0	26.610	1.012
623.9	24.0	26.890	1.010

TABLE VI (CONTINUED)

Core Burnup (MWd)	Equilibrium Power (MW)	Shim Rod Bank Height (in)	Rods-Out Reactivity k_{eff}
647.9	24.0	27.200	1.008
659.6	24.0	27.325	1.007
659.6	0	22.171	1.048
680.0	12.0	26.750	1.011
686.0	12.0	26.910	1.010
690.0	12.0	26.945	1.010
717.7	12.0	27.050	1.009
723.7	12.0	27.165	1.009
748.2	12.0	27.301	1.008
754.2	12.0	27.450	1.007
760.2	12.0	27.591	1.007
766.2	12.0	27.650	1.006
772.2	12.0	27.730	1.006
778.2	12.0	27.825	1.005
780.2	12.0	27.860	1.005
780.2	0	23.350	1.037
805.6	12.0	28.300	1.004
817.5	12.0	28.500	1.003
823.5	12.0	28.675	1.003
829.5	12.0	28.800	1.002
833.5	12.0	28.875	1.002
833.5	0	23.150	1.038
849.6	12.0	28.975	1.002
855.6	12.0	29.550	1.001
859.7	12.0	29.660	1.001
884.6	12.0	29.800	1.000

V. ZERO POWER EXPERIMENTS AT STEPS DURING BURNUP

A. Rod Calibrations

Shim rod differential worth measurements were performed at two steps during the burnup of the MTR-Phoenix core, in addition to those performed before burnup commenced. One set of measurements was performed at a core burnup of 660 MWd, the other at 834 MWd. Since, as we have seen in the previous section, the critical rod bank height moved up as core burnup progressed, these later differential measurements were not made at a height of 18 in.

The results of the three sets of shim rod differential worth measurements are presented in Table VII. They are also presented graphically in Figure 18.

TABLE VII

SHIM ROD DIFFERENTIAL WORTHS

Shim Rod Position	Rod Differential Worths* (¢/in.)		
	0 MWd Ht = 18.0 in.	660 MWd Ht = 22.1 in.	834 MWd Ht = 23.0 in.
L-22	61.6	33.7	29.2
L-42	61.8	35.7	32.0
L-24	91.0	50.3	47.2
L-44	91.4	50.0	47.2
L-26	92.2	43.3	46.9
L-46	90.6	40.5	47.8
L-28	45.7	27.0	27.3
L-48	58.6	28.0	23.3
Total	592.9	308.5	300.9

*All worths quoted have an uncertainty of ± 2%.

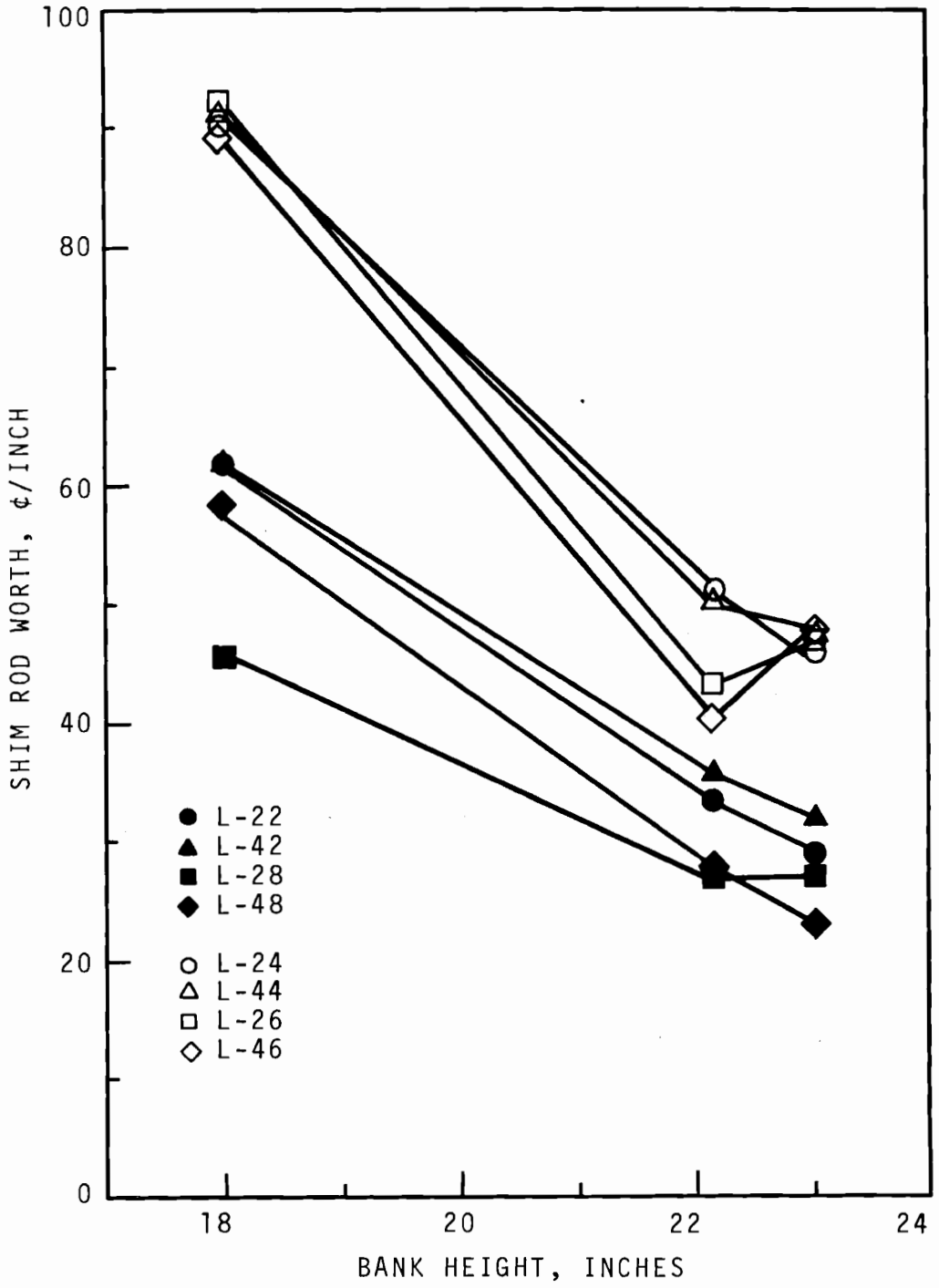

FIGURE 18. Shim Rod Differential Worths Vs. Rod Bank Height: MTR-Phoenix Core

The later differential worth measurements may be compared with those made initially by differentiating the rod bank worth curve of Figure 6 at the appropriate heights. These data appear in Table VIII.

TABLE VIII

Change in Shim Rod Worth with Burnup

	Bank Differential Worth ($/in.)	
	H = 22.1 in.	H = 23.0 in.
From integral worth curve measured initially	3.93	3.36
Measured at 660 MWd	3.09	--
Measured at 834 MWd	--	3.01

A decreasing rod worth with burnup is observed.

B. Kinetics Measurements

Reactor noise measurements, as described in Section IV.E, were repeated near the end of the MTR-Phoenix core lifetime. Fission chamber data were recorded with the reactor operating at 10 kw. The spectrum obtained is shown in Figure 19. The analysis of this spectrum yielded a best estimate of β/ℓ of 9.34 ± 0.50 Hz. The reason for the relatively poor estimate of β/ℓ is apparent from Figure 19. Two factors contributed to the 5% uncertainty. First, the low efficiency of the fission chambers did not yield the ratio of correlated-to-uncorrelated signals necessary for a good estimate. Second, flow noise apparently existed in the 8 to 10 Hz frequency range.

Within the experimental uncertainties, one may conclude that the value of β/ℓ for the MTR-Phoenix core did not change with burnup.

C. Neutron Flux Spectrum Measurements

Measurements were made of the neutron spectrum of the MTR-Phoenix core at the end of its burnup lifetime. A multiple foil activation technique utilizing the SPECTRA code for data analysis was used. The SPECTRA code provides a neutron flux spectrum that minimizes an error function. A trial spectrum is supplied as tabular input, and by requiring that the squared difference between the measured and calculated detector activities be a part of the function, it is possible to obtain a convergence fit to the new spectral shape.

The two locations within the core where the measurements were made were channel No. 8 of L-35, and channel No. 8 of L-45. Each location had two measurement positions; one position was four inches down from the top of the

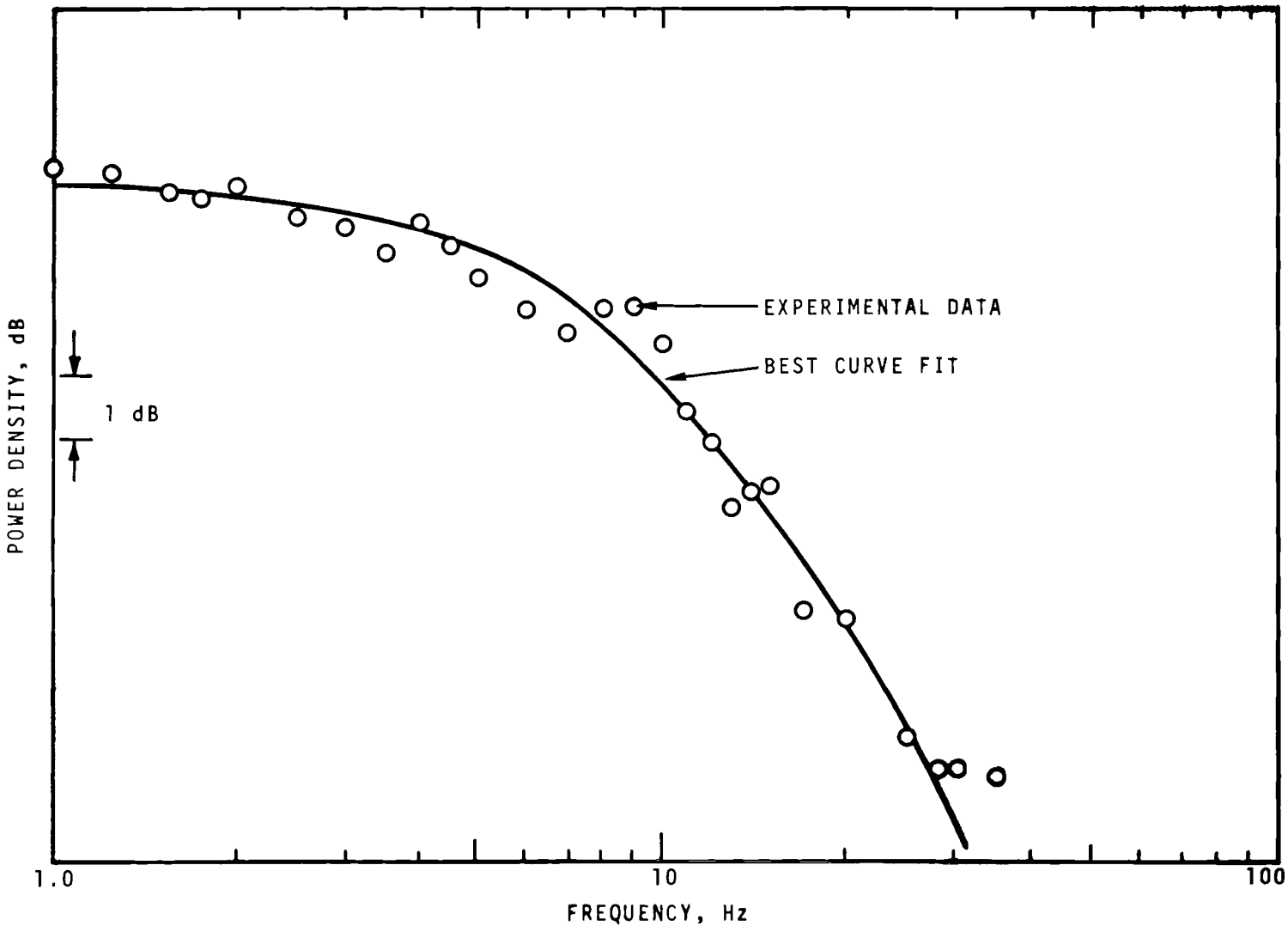

FIGURE 19. Cross Power Noise Spectrum: MTR-Phoenix Core with a Burnup of 907 MWd

fuel plate, and the other position was sixteen inches down from the top of the fuel plate. This arrangement gave a total of four measurement positions.

Aluminum wands with suitable foil packets were fabricated such that when the wands were inserted, the packets were at the above described positions. For each position, $^{55}Mn\ (n,\gamma)^{56}Mn$, $^{63}Cu(n,\gamma)^{64}Cu$, $^{45}Sc(n,\gamma)^{46}Sc$, $^{50}Cr(n,\gamma)^{51}Cr$, $^{64}Zn(n,p)^{64}Cu$, $^{58}Ni(n,p)^{58}Co$, $^{54}Fe(n,p)^{54}Mn$, $^{46}Ti(n,p)^{46}Sc$, $^{24}Mg(n,p)^{24}Na$, and $^{27}Al(n,\alpha)^{24}Na$ were used.

After insertion of the aluminum wands with the foil packets, the reactor was brought to a power of 400 kw and retained at this level for two hours before being scrammed. The activated foils were then removed from the wands, and after a suitable waiting period, were counted on both a Na(I) and a Ge(Li) multi-channel analyzer to determine their induced activity.

The measured neutron flux values at specified neutron energies are listed in Table IX for the locations in fuel elements 35 and 45. The cadmium ratios for ^{59}Co and the 2200 m/sec thermal-neutron fluxes are tabulated in the last two columns.

TABLE IX

Measured Neutron Fluxes

Location	Neutron Energy					R_{cd}	ϕ_{th}-n/cm^2/sec
	0.654 eV	4.91 eV	21.6 eV	132 eV	514 eV		
	Neutron Flux - n/cm^2/sec/eV						
Fe-35-Top	1.56×10^{11}	3.02×10^{10}	7.54×10^{9}	1.21×10^{9}	3.10×10^{8}	2.3	3.0×10^{11}
Fe-35-Center	4.63×10^{11}	8.47×10^{10}	2.20×10^{10}	3.67×10^{9}	9.34×10^{8}	2.0	7.8×10^{11}
Fe-45-Top	1.33×10^{11}	2.58×10^{10}	6.54×10^{9}	1.02×10^{9}	2.88×10^{8}	2.9	3.4×10^{11}
Fe-45-Center	4.34×10^{11}	8.02×10^{10}	2.01×10^{10}	3.49×0^{9}	8.82×10^{8}	2.6	9.9×10^{11}

Corrections were made for the contributions to the activities by higher energy resonances when necessary. Self-shielding by detector atoms in the samples were less than 1%.

Using a calculated initial trial spectrum, and the measured activities from the foils, a core spectrum for each position was determined. The comparative results between the calculated and measured spectra in locations L-35 and L-45 are shown in Figures 20 and 21 respectively.

Good agreement between calculated and measured spectra is seen for energies less than 1 MeV. In the few MeV region, the measured flux is about 10% higher than that calculated. The source of this anomaly is being investigated.

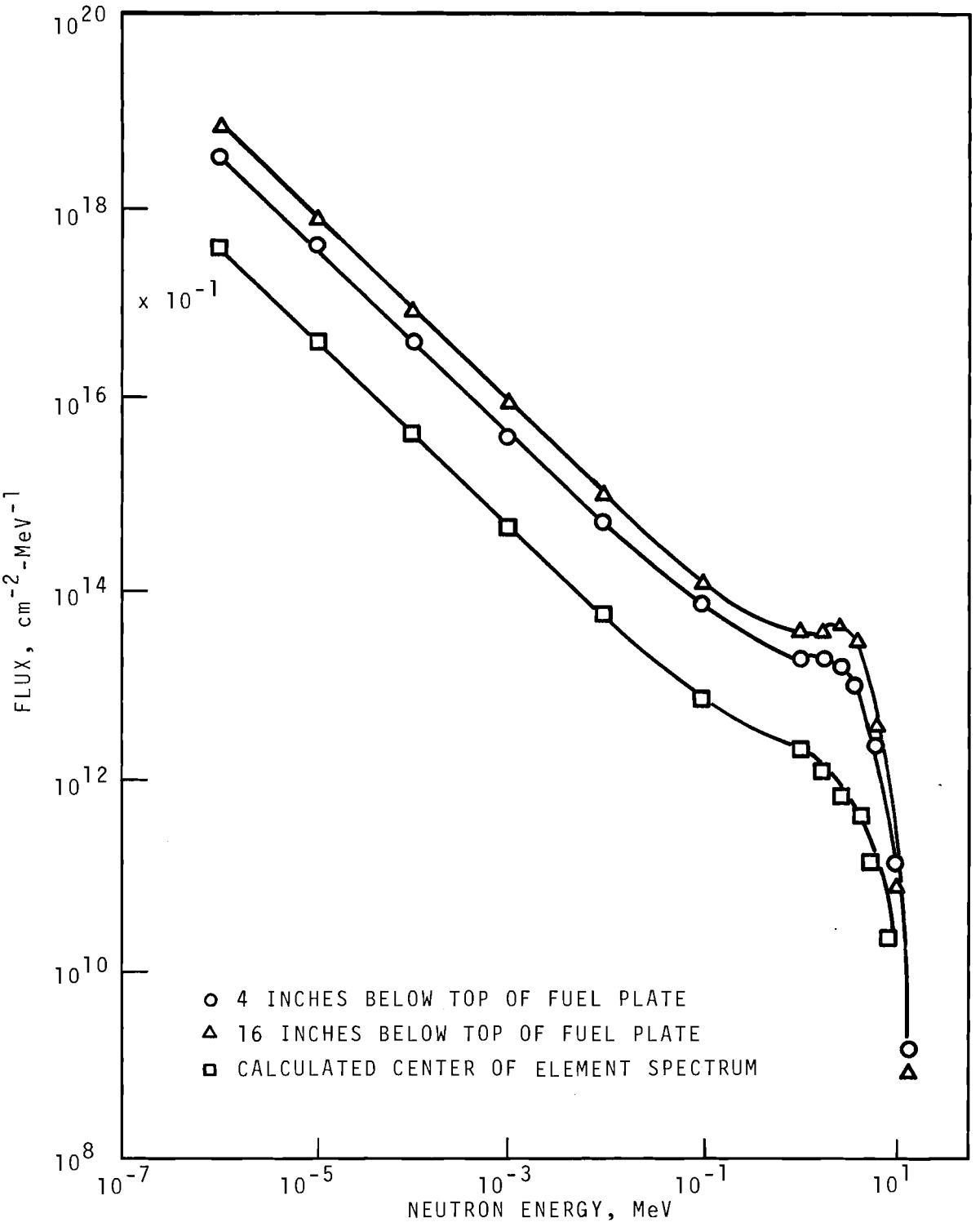

FIGURE 20. Neutron Flux Spectrun in Water Channel 8 of Core Position L-35: MTR-Phoenix Core

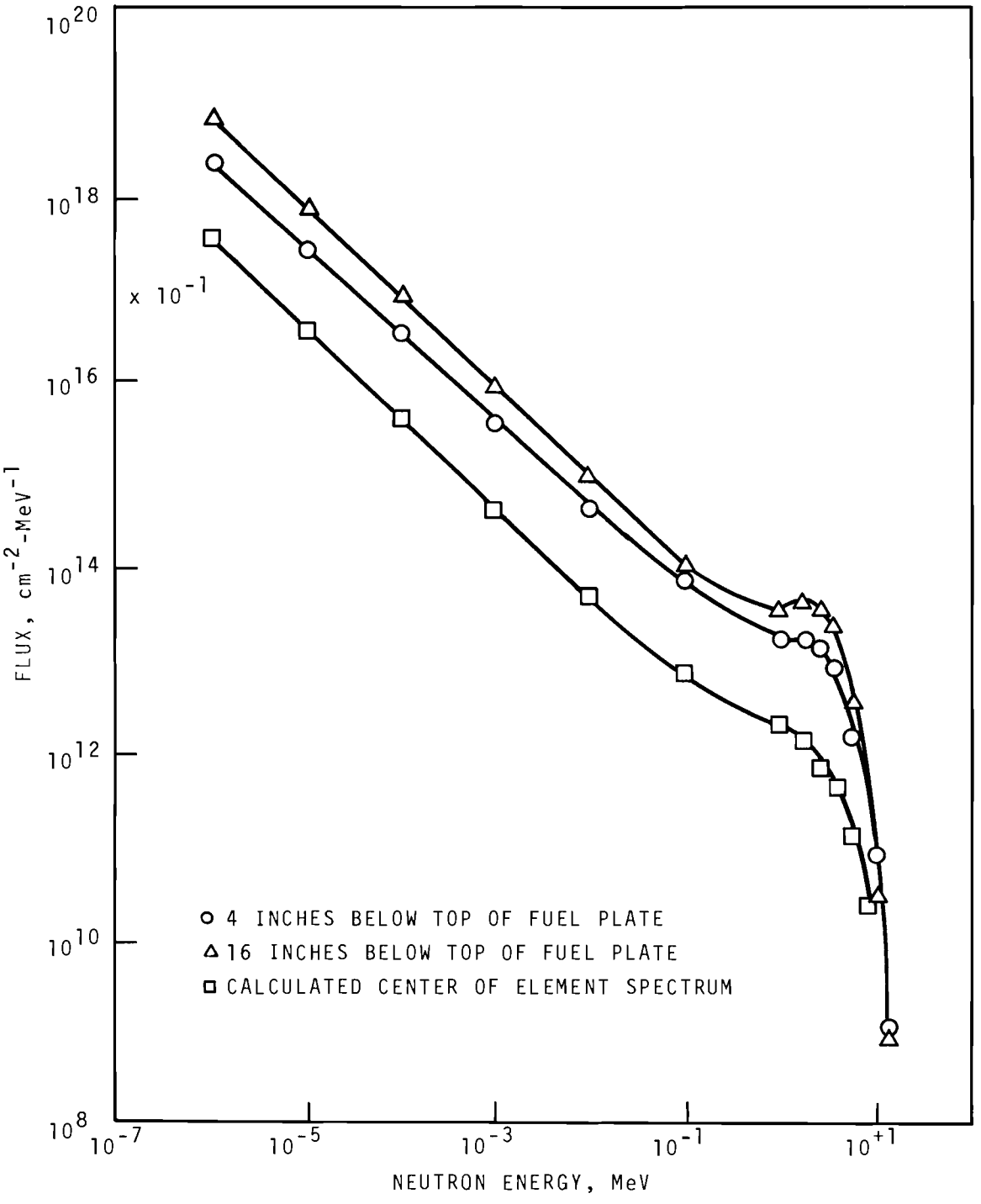

FIGURE 21. Neutron Flux Spectrum in Water Channel 8 of Core Position L-45: MTR-Phoenix Core

ACKNOWLEDGEMENTS

Many people, both at Battelle and at Idaho Nuclear Corporation, participated in the planning, performance, and analysis of the MTR-Phoenix Fuel Experiment. While it is impossible to acknowledge the contributions of all these people, a few individuals are singled out for special recognition.

In the planning stage, important contributions were made at Battelle by G.J. Busselman, D.D. Lanning, L.C. Schmid, and R.I. Smith, and at INC by E.E. Burdick, D.R. deBoisblanc, N.C. Kaufman, and R.S. Marsden. Fuel design and fabrication were handled ably by R.G. Curran and W.L. Hampson at BNW.

All the measurements reported here were performed by MTR Operations personnel of Idaho Nuclear Corporation. The reduction of reactor period data to reactivity values and the analysis of the kinetics measurements and neutron spectrum measurements were performed by INC personnel. We are grateful to them for providing us with both the raw data and the inferred reactivity values. Special thanks go to N.C. Kaufman for his unstinting efforts throughout the entire experiment.

In the data analysis at Battelle, we acknowledge the contributions of G.J. Konzek, R.A. McBride, and G.R. Monk in reducing the power distribution measurement data to meaningful form. W.P. Stinson performed the noise analysis at Battelle in parallel with the INC work.

Analytical correlations of the MTR-Phoenix Fuel Experiment have been performed by C.M. Heeb[5] and U.P. Jenquin.[9] Their contributions to the planning and analysis of specific measurements are gratefully acknowledged.

REFERENCES

1. P.L. Hofmann, G.J. Busselman, and R.H. Holeman, Nuclear Characteristics of Some Compact, Water Moderated, Plutonium Burners, HW-79977, Hanford Laboratories (1964).

   R.H. Holeman and P.L. Hofmann, Nuclear Design Calculations for a Hx-Pu Fueled MTR, HW-84575, Hanford Laboratories (1964).

2. D.G. Albertson and G.J. Busselman, "Analysis and Measurement of Pu Al-Polyethylene Systems in the PCTR," Trans. Am. Nucl. Soc., 8, 448 (1965).

3. W.P. Stinson and C.M. Heeb, "Approach-to-Critical Experiments with Phoenix Fuel," Trans. Am. Nucl. Soc., 10, 187 (1967).

4. E.C. Davis, R.I. Smith, and L.D. Williams, Critical Experiments in an MTR Mockup Using Phoenix Fuel, BNWL-1481, Pacific Northwest Laboratories (1970).

5. C.M. Heeb, Analysis of the Phoenix Fuel Experiments, BNWL-1514, Pacific Northwest Laboratories (1970).

6. R.J. Nertney et al, Fundamentals in the Operation of Nuclear Test Reactors, Volume 2, Materials Testing Reactor Design and Operation, IDO-16871-2, Phillips Petroleum Company (1963).

7. R.S. Marsden, R.L. Curtis, and D.W. Knight, Safety Analysis Report for the MTR Phoenix Fuel Experiment, IN-1209, Idaho Nuclear Corporation (1969).

8. Idaho Nuclear Corporation, unpublished data.

9. U.P. Jenquin et al, Burnup Calculations and Post Irradiation Fuel Analysis for the MTR-Phoenix Fuel Experiment, to be published.

APPENDIX

Fuel Plate Axial Gamma Scans

The results of all the full-width axial plate scans performed in the MTR-Phoenix experiment appear in Figures A-1 through A-8. In each case the tapered bottom end of the fuel plate is shown. All data are normalized to core average power.

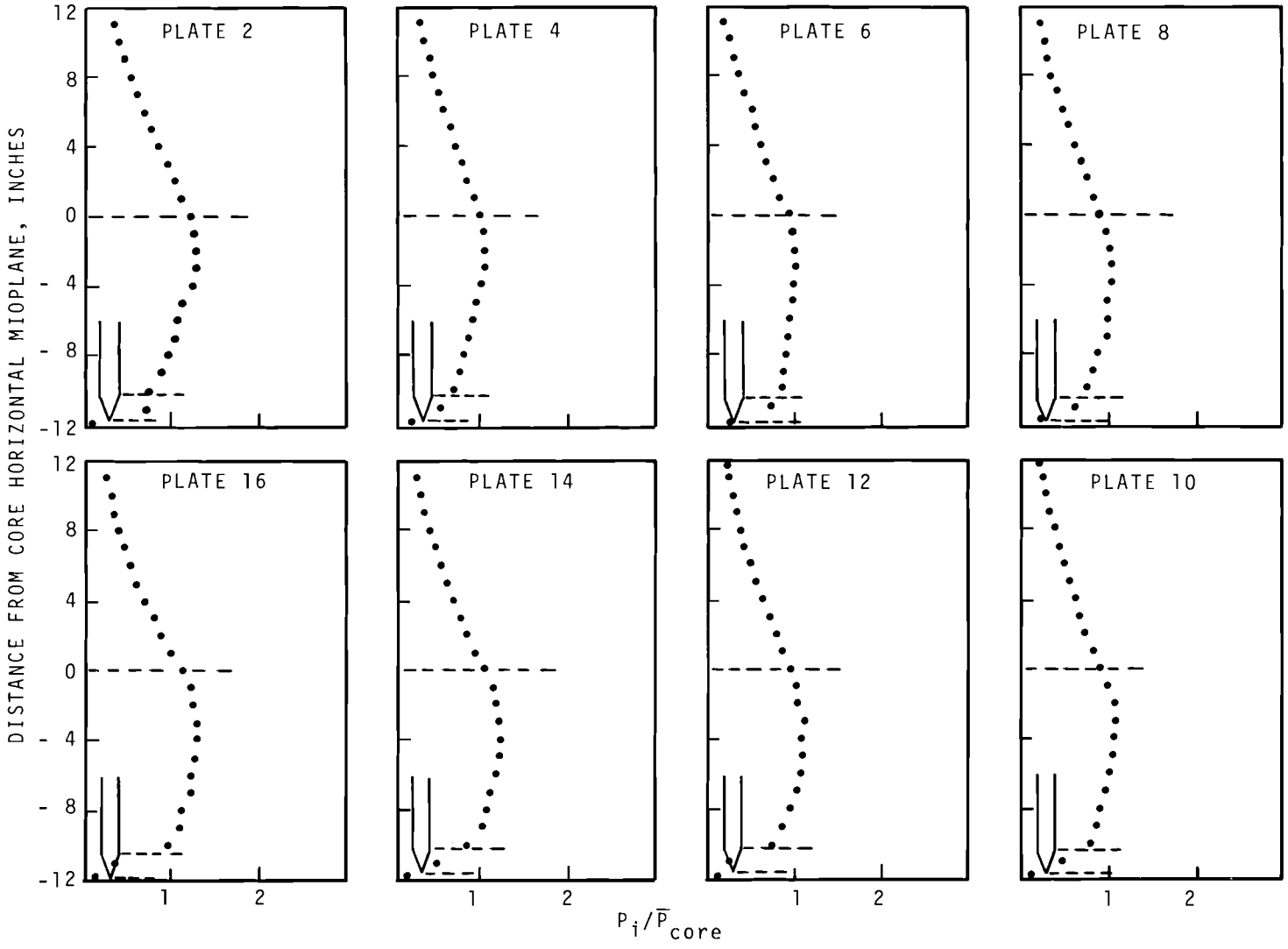

FIGURE A-1. Full-Width Axial Gamma Scans of Eight Plates from Fuel Element Position L-31

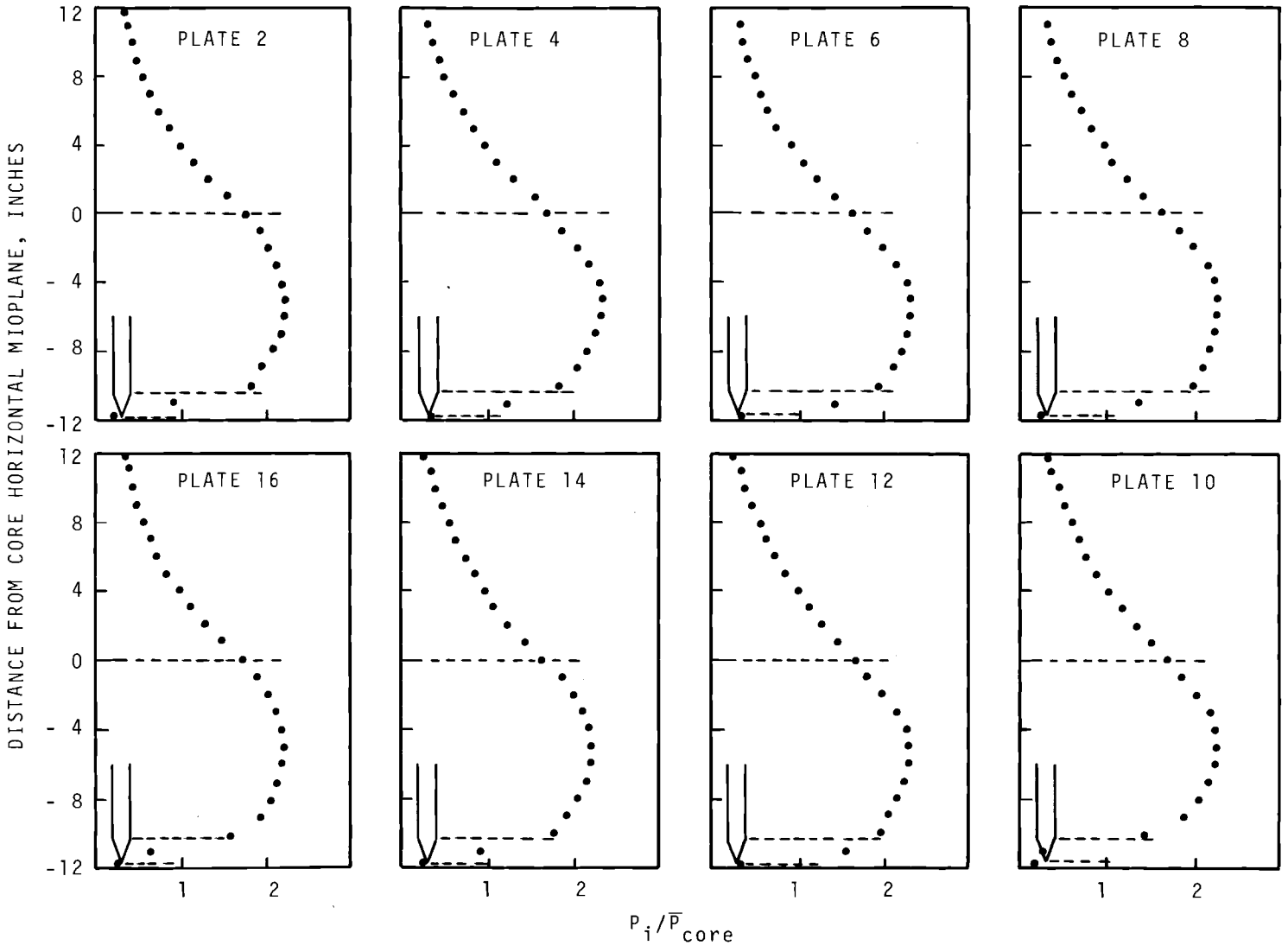

FIGURE A-2. Full-Width Axial Gamma Scans of Eight Plates from Fuel Element Position L-35

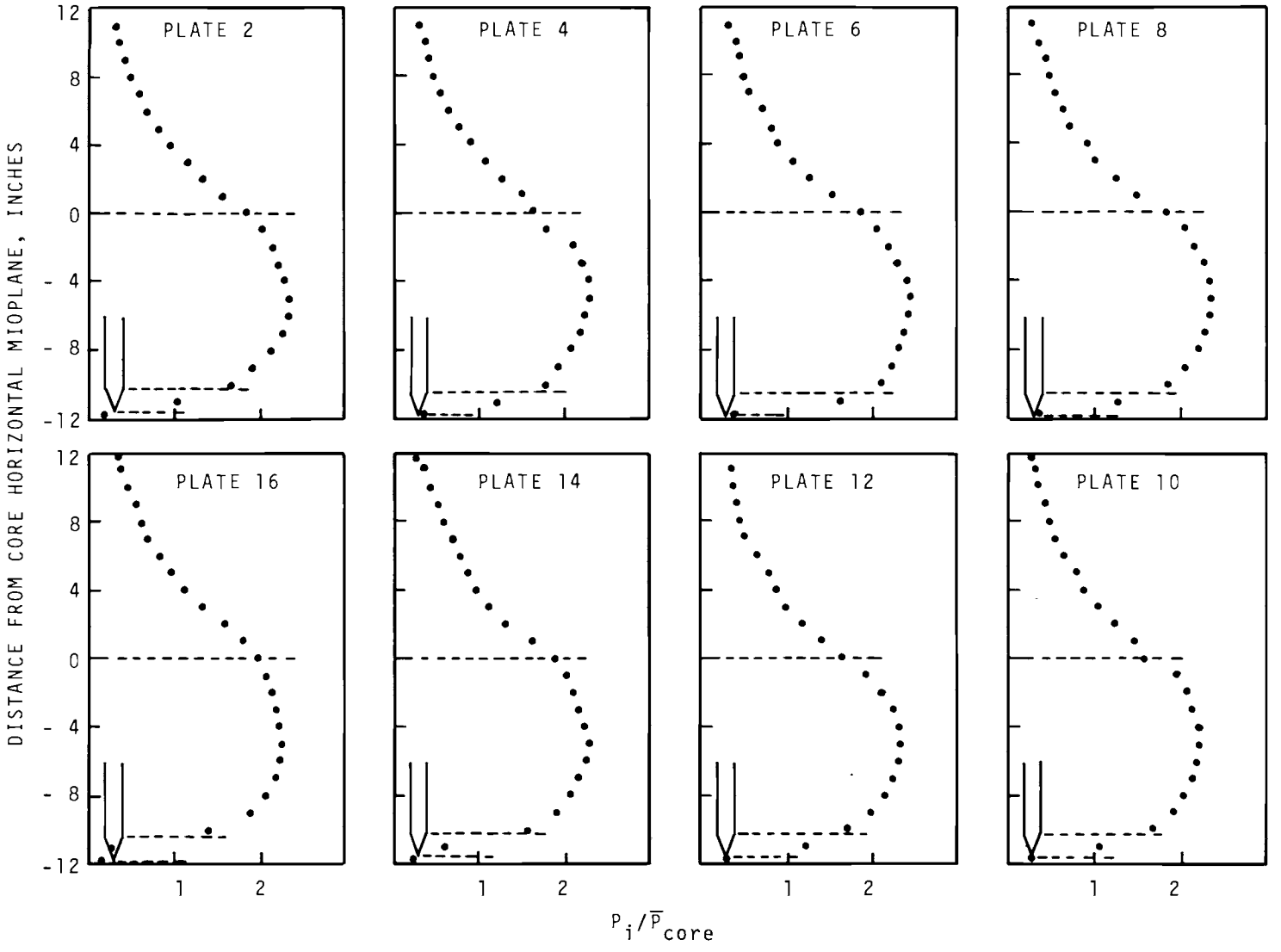

FIGURE A-3. Full-Width Axial Gamma Scans of Eight Plates from Fuel Element Position L-36

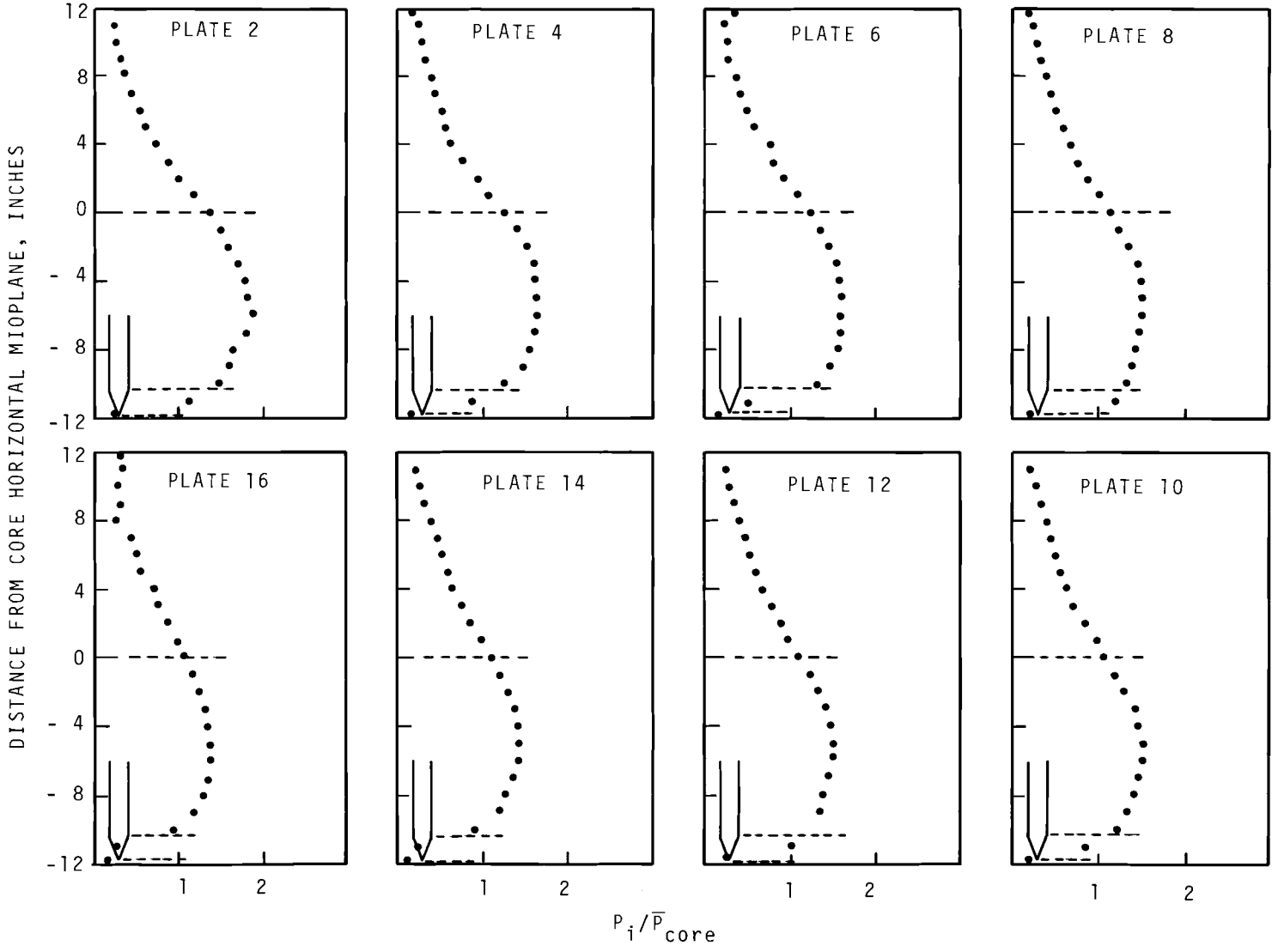

FIGURE A-4. Full-Width Axial Gamma Scans of Eight Plates from Fuel Element Position L-37

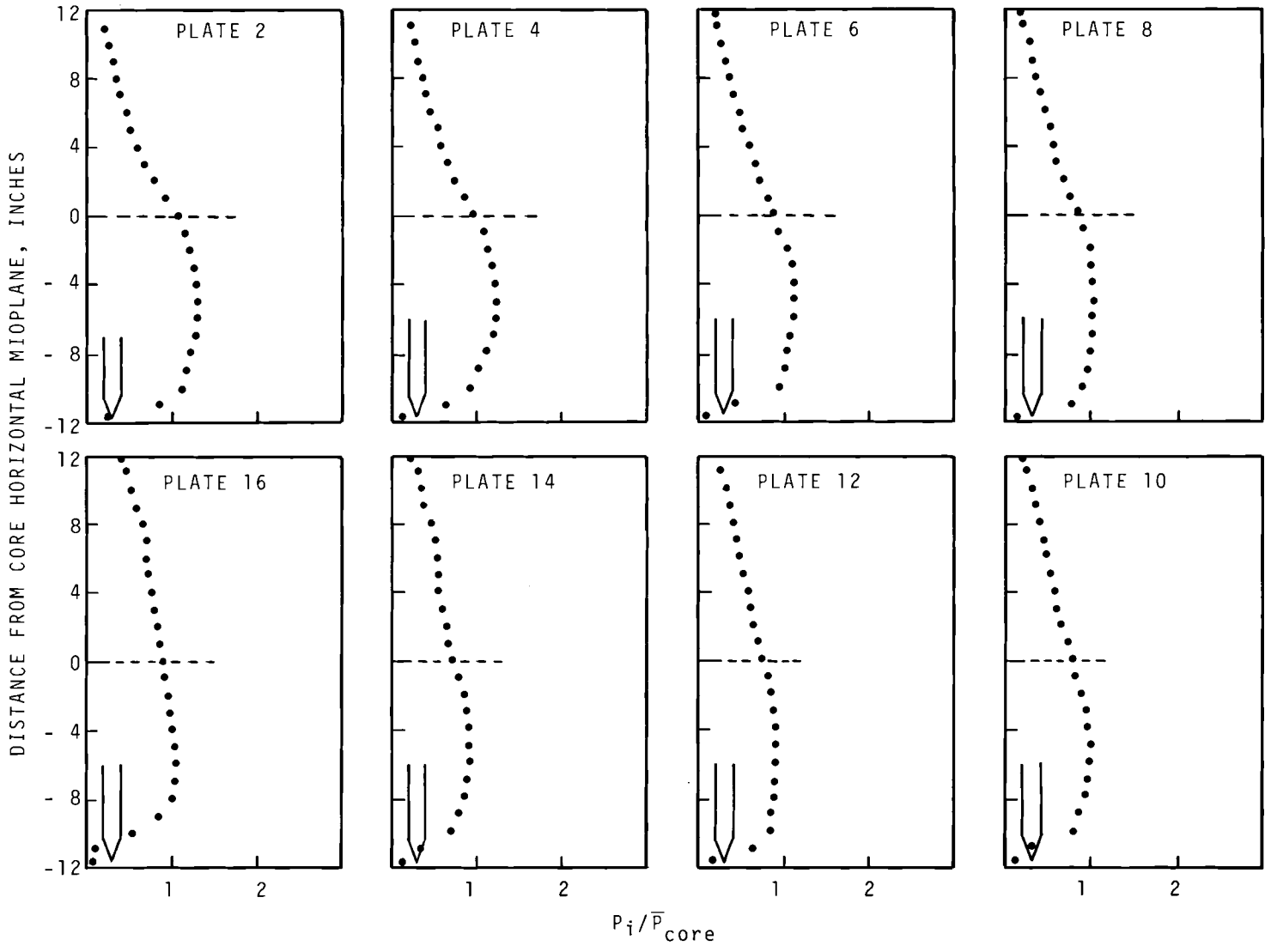

FIGURE A-5. Full-Width Axial Gamma Scans of Eight Plates from Fuel Element Position L-39

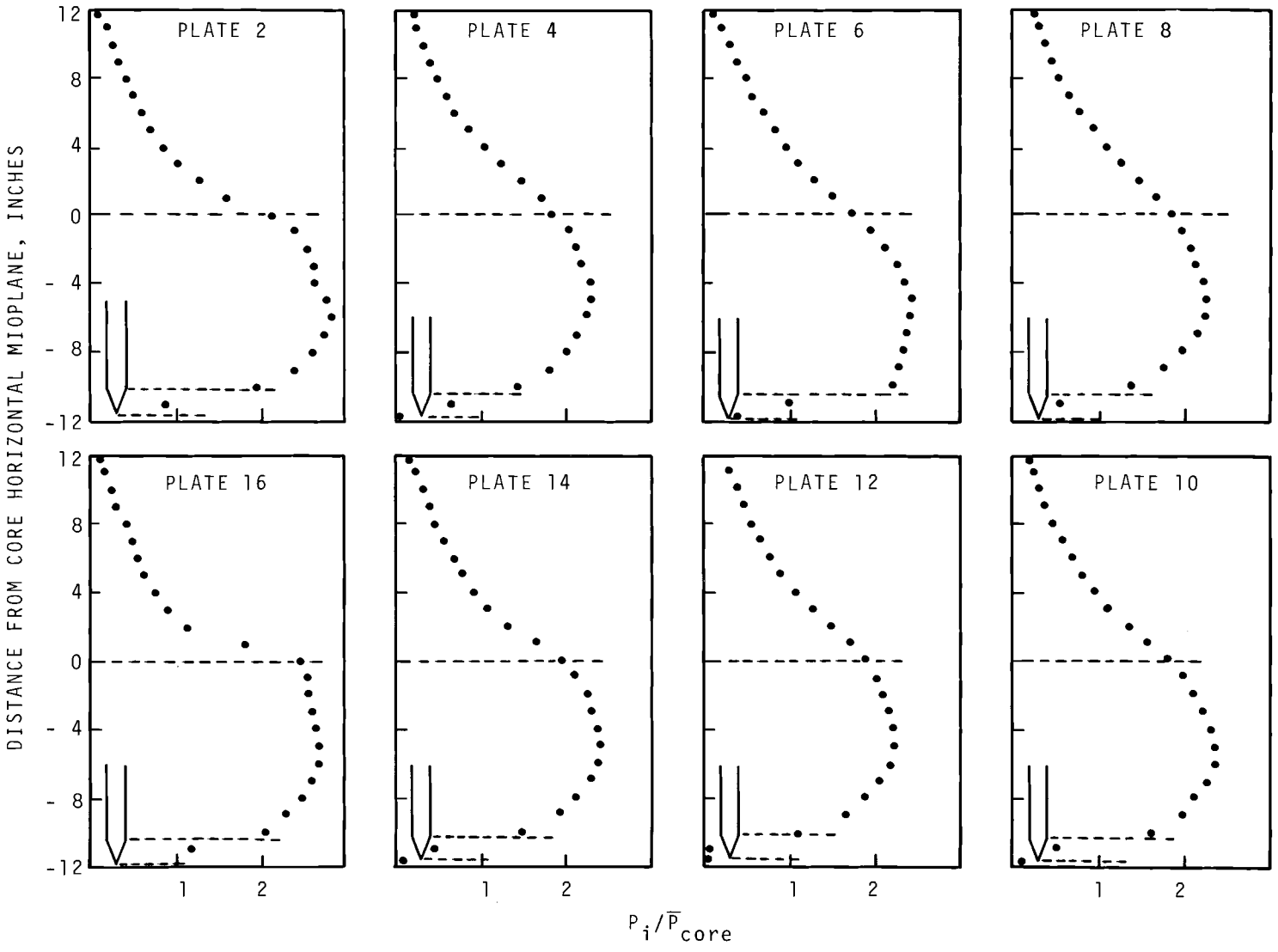

FIGURE A-6. Full-Width Axial Gamma Scans of Eight Plates from Fuel Element Position L-45

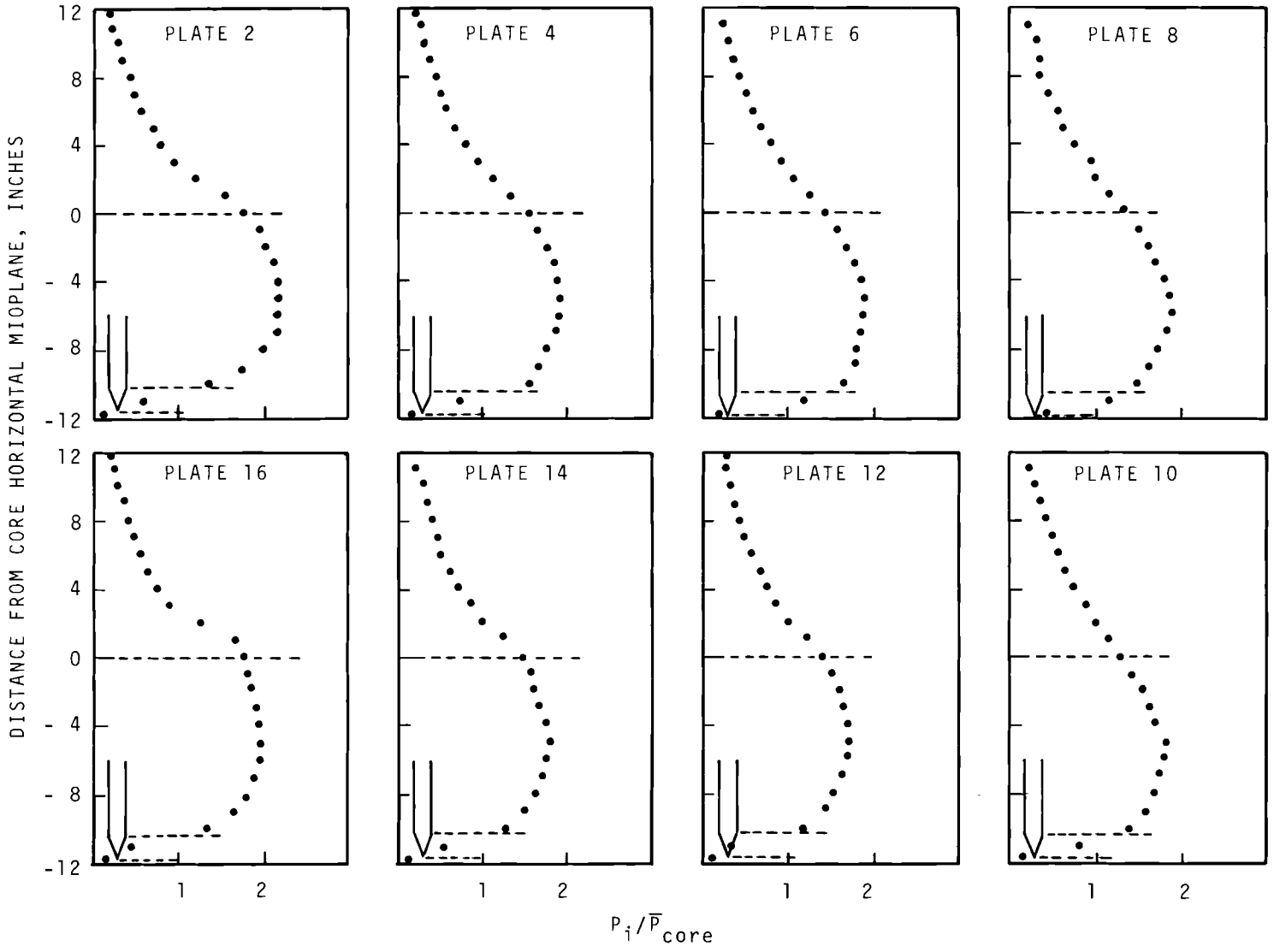

FIGURE A-7. Full-Width Axial Gamma Scans of Eight Plates from Fuel Element Position L-47

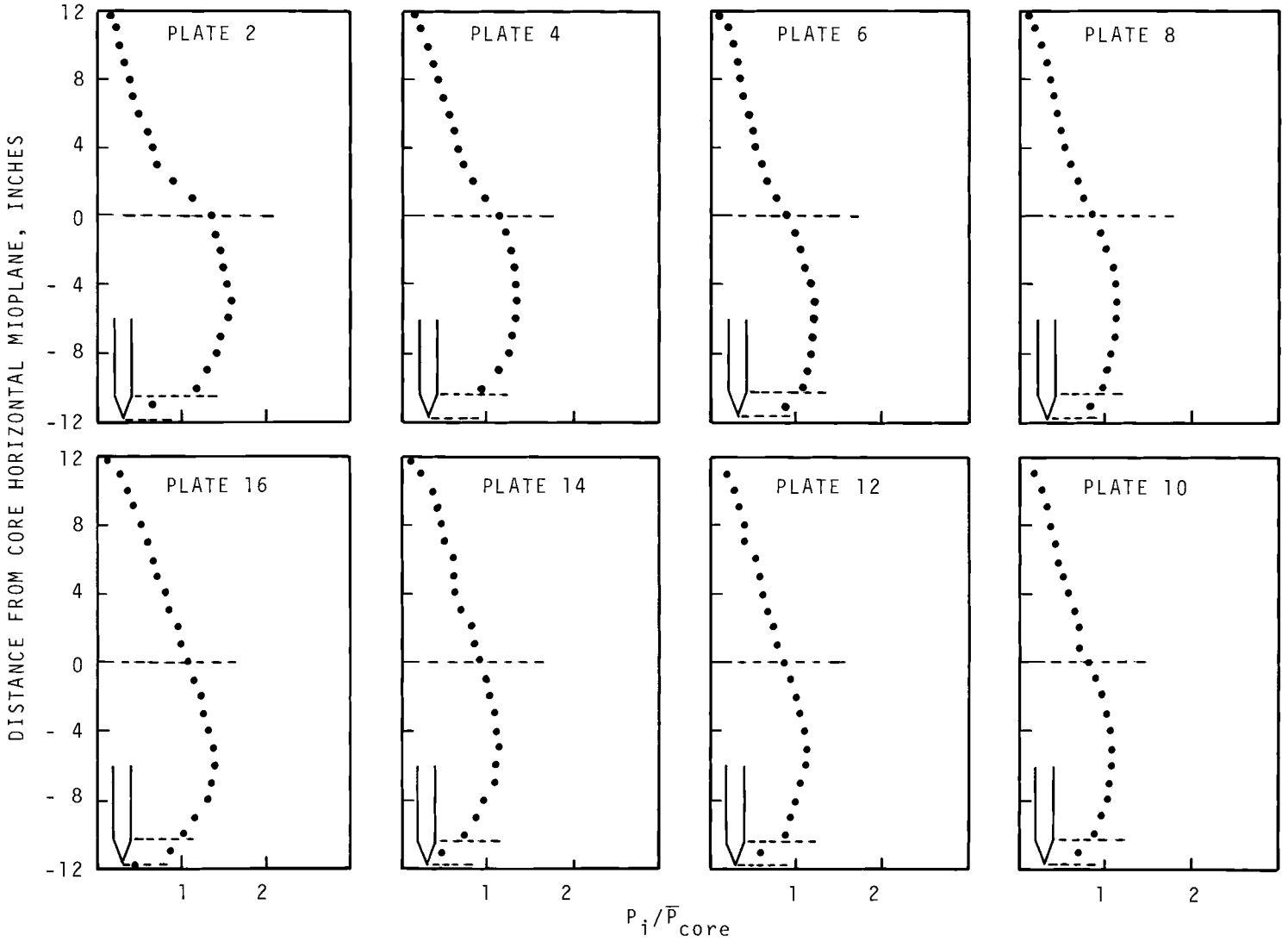

FIGURE A-8. Full-Width Axial Gamma Scans of Eight Plates from Fuel Element Position L-49

BNWL-1593
Special Distribution
in Category UC-80

No. of Copies

OFFSITE

1 AEC Chicago Patent Group

G. H. Lee

7 AEC Division of Reactor Development and Technology

Director, RDT
Asst. Dir., Project Management
Chief, Water Projects Branch (2)
Asst. Dir., Reactor Technology
Chief, Reactor Physics Branch (2)

AEC Division of Technical Information Extension

3 Argonne National Laboratory

R. Avery
C. H. Bean
R. E. Machery

1 Atomic Energy of Canada Limited

Chalk River Nuclear Laboratory
Reactor Physics Branch
Chalk River, Ontario, Canada

M. Duret

1 Babcock and Wilcox

P. O. Box 1260
Lynchburg, VA 24505

H. M. Jones

1 Bhabha Atomic Research Centre

Theoretical Physics Section/RED
Central Complex Bldg.
Trombay, Bombay-85, India

S. R. Dwivedi

No. of Copies

1 Brookhaven National Laboratory

G. Price

3 Combustion Engineering

P. O. Box 500
Windsor, Connecticut 06095

R. Harding
R. Hellens
S. Visner

1 Commonwealth Edison Company

72 West Adams Street
Chicago, Ill.

A. Veras

1 Consumers Power Company

1945 W. Parnall Road
Jackson, Mich. 49201

G. J. Walke

2 CNEN - Centro Studi-Nuclearie

Casaccia, Rome, Italy

Ugo Farinelli
Paolo Loizzo

1 EBASCO Services

2 Rector St.
New York, N. Y. 10006

D. deBloisblanc

No. of Copies

2 Edison Electric Institute
750 Third Avenue
New York, N. Y. 10017

John J. Kearney
George Watkins

2 E. I. de Pont deNemours & Company, Inc., SRL

G. Dessauer
H. Honeck

1 ENEL
Via G. B. Martini
(Pizaaz Verdi)
Rome, Italy

Mr. Paloetti Gaulandi

5 Florida Power and Light
Miami, Florida

E. C. Davis (5)

2 General Electric Co., San Jose
Nuc. Dev. and Eng.
175 Curtner Avenue
San Jose, California 95112

D. L. Fischer
R. L. Crowther

2 General Electric Co., Vallecitos Atomic Lab.
P. O. Box 846
Pleasanton, California 94566

D. G. Albertson
T. M. Snyder

No. of Copies

7 Idaho Nuclear Corporation

R. M. Brugger
E. E. Burdick
N. C. Kaufman (5)

1 Japan Atomic Energy Institute

TCA-JPDR
Tokai-Mura, Naka-Gun, Ibaraki-Ken
Japan

Shojiro Matsuura

1 Kerr-McGee

Kerr-McGee Bldg.
133 NW Robert S. Kerr Ave.
Oklahoma City, Okla. 73102

Dr. Frank Pittman

1 Massachusetts Institute of Technology

1338 Albany Street
Bldg. NW 12
Cambridge, Mass. 02139

D. D. Lanning

1 Nuclear Materials and Equipment Corp.

Penn Center
Apollo, Penn. 15613

K. Puechl

1 NUKEM

D-645, HANAU
POSTFACH 869
Germany

Mr. Wolgang K. L. Jager

No. of Copies

1 Pakistan Institute of Nuclear Sci. & Tech.

P. O. Nilore
Rawalpindi, Pakistan

M. A. Mannan

1 Philadelphia Electric Company

1000 Chestnut Street
Philadelphia 5, Pa.

Mr. Wayne C. Astley

1 Power Reactor & Nuclear Fuel Development Corp.

9-13, 1- chome, Akaska
Minato-ku, Tokyo, Japan

Setsuo Kobayashi

1 S. C. K. - C. E. N.

MOL-DONK
Belgium

Dr. H. Vanden Broeck
BRL.

1 United Nuclear Corporation

Research & Engineering Center
Grasslands Road
Elmsford, New York 10523

J. R. Tomonto

4 Westinghouse Electric Corporation

Atomic Power Division
Post Office Box 355
Pittsburgh, Penn. 15230

R. J. French
R. S. Miller
W. L. Orr
J. R. Worden

ONSITE

1 AEC Chicago Patent Group

R.M. Poteat (Richland)

No. of Copies

5 RDT Assistant Director for Pacific Northwest Programs

W. E. Fry
P. G. Holsted
J. B. Kitchen
T. A. Nemzek (2)

2 AEC Richland Operations Office

H. A. House
M. R. Schneller

5 Douglas United Nuclear

C. D. Harrington
C. W. Kuhlman
DUN Files (3)

6 WADCO Corporation

R. A. Bennett
E. M. Heck
R. E. Heineman
P. L. Hofmann
K. R. Wise
WADCO Document Control

76 Battelle-Northwest

J. M. Batch
C. A. Bennett
S. H. Bush
J. L. Carter
N. E. Carter
D. E. Christensen
F. G. Dawson
D. E. Deonigi
L. J. Federico
J. C. Fox
M. D. Freshley
S. Goldsmith
C. M. Heeb
H. L. Henry
R. M. Hiatt
R. S. Hope
(BNW, Idaho Falls)
U. P. Jenquin
B. M. Johnson
G. J. Konzek
D. A. Kottwitz
J. W. Kutcher (25)
D. C. Lehfeldt
B. R. Leonard
R. C. Liikala
C. W. Lindenmeier
D. F. Newman
D. R. Oden
H. M. Parker
R. S. Paul
L. T. Pedersen
W. W. Porath
D. L. Prezbindowski
W. L. Purcell

No. of
Copies

Battelle-Northwest (contd.)
W. D. Richmond
G. D. Seybold
L. C. Schmid
R. I. Smith
D. H. Thomsen
V. O. Uotinen
R. G. Wheeler
L. D. Williams
N. G. Wittenbrock
W. C. Wolkenhauer
F. R. Zaloudek
M. G. Zimmerman
Technical Information (5)
Technical Publications (2)